Comparison analysis of Bacillus Calmette-Guerin induced Autophagy mechanisms in Macrophages Derived from Human Induced Pluripotent Stem Cells and THP-1

Mengyi Zhu
Zhejiang Sci-Tech University
Danping Hong
Zhejiang Sci-tech University
Ouyang Li
Zhejiang Sci-Tech University
Ahmed Salah Hassan
Zhejiang Sci-Tech University
Yanqin Li
Zhejiang Sci-Tech University
Nafee-ul Alam
Zhejiang Sci-Tech University
Wen-Bin Ou
Zhejiang Sci-Tech University
Yuehong Wu (wuyuehong2003@163.com)
College of life science, Zhejiang Sci-Tech University

Research

Keywords: hiPS-Mφ, Mycobacterium tuberculosis infection, Tuberculosis, BCG, transcriptome, autophagy, PI3K/AKT/mTOR signaling pathway

Posted Date: May 8th, 2020

DOI: https://doi.org/10.21203/rs.3.rs-26931/v1

Abstract

Background Tuberculosis (TB) remains a major global public health problem and the leading cause of mortality by a single infectious agent. TB is a chronic infectious disease that is primarily caused by Mycobacterium tuberculosis (Mtb). Macrophage (Mφ) are the main hosts of Mtb, the interaction between Mtb and Mφ plays an important role in the pathogenesis of TB.

Summary The macrophages used in the current study are mostly derived from tumor cell lines or peripheral blood mononuclear cells (PBMC), but the application of such cells still have many problems needed to be sloved, such as the loss of function due to changes in genetic structure and the difficulty in cell acquisition. Human induced pluripotent stem cells (hiPS) represent an innovative source for the standardized *in vitro* generation of Mφ, and show novel promise in exploring disease pathogenesis, particularly TB. Current studies have revealed that autophagy plays a central role in the interaction between Mtb and Mφ, but the molecular mechanism involoved remains unclear and the exact role of hiPS-derived macrophages (hiPS-Mφ) in regulating autophagy induced by Mtb also remains unclear. To investigate the similarities and differences in hiPS-Mφ and THP-1-Mφ in anti-tuberculosis immunity, this study successfully obtained macrophages derived from hiPS and THP-1, then explored the mechanism behind Bacillus Calmette-Guerin (BCG)-induced autophagy through transcriptome sequencing analysis, qPCR, Western Blot Analysis and cell submicroscopic structure observation etc.. Our findings revealed that BCG infection of hiPS-Mφ and THP-1-Mφ would promote autophagy by regulating the expression of autophagy-related genes, which also indicated that the BCG-induced autophagy in hiPS-Mφ and THP-1-Mφ may be associated with PI3K/AKT/mTOR signaling pathway. However, there are some differences in the mechanism by which BCG infects macrophages from different sources and induces autophagy. Considering the above findings, we have provided novel insights into the role of macrophages along with autophagy in the anti-tuberculosis immune mechanism and the possibility of establishing an *in vitro* hiPS-Mφ-TB disease model.

1. Introduction

Macrophages (Mφ) are present in all tissues of mammals. As a key component of the innate immune system, macrophages exhibit extremely significant plasticity and play an important role [1–4], for example, eliminating invading pathogens, remodeling tissues and clearing dead cells[5]. Macrophages are associated with various types of cancer in terms of tumors [6–9], and in the aspect of cardiovascular diseases, atherosclerosis and metabolic regulatory abnormalities are also closely related to it [10,11]. In summary, it is not difficult to see the significance of macrophages in human health issues. Unfortunately, normal human macrophages (e.g. blood monocyte derived macrophages, bone-marrow derived macrophages) are too difficult to be acquired and they cannot self-renew, hindering the development of relevant researches. More importantly, each study requires large amounts of cells, which means we will require large amounts of blood from the donors and it may cause ethical issues. The differences of donors' physiological state and genes are also a tough problem, making the test results to be not

representative. To solve all these problems, the macrophages currently used for immunological researches are RAW264.7 along with cells derived from tumor cell lines (e.g. U937, THP-1) and primary cells (e.g. tissue cells and PBMC). Among them, RAW264.7 is a mouse-specific macrophage, while U937-Mφ and THP-1-Mφ are both derived from tumor cell lines, the main differences between these two sources are the origin and the maturity stage. U937 cells are of tissue origin and therefore at a more mature stage while THP-1 cells originate from hematological leukemia cells and belong to a less mature stage[12]. Although they are all immortalized cell lines and can be cultured *in vitro* to the 25th generation, maintaining cell sensitivity and activity, THP-1 cells are more suitable for further researches as the growth rate of THP-1 increases faster, more importantly, there are no reports related to the infectious viruses or toxic products in these cells. Such a cell line is relatively easy and safe. Due to the homologous genetic background, the degree of change in cell phenotype is minimized, which is conducive to experimental reproducibility[13,14]. But cells derived from these sources still have various defects, such as being difficult to obtain and manipulate, furthermore they are also prone to mutations.

In 2006, induced pluripotent stem cells (iPS) were obtained by Japanese scientists Takahashi and Yamanaka, who introduced four transcription factors (*OCT4*, *SOX2*, *KLF4, c-MYC*) into mouse skin fibroblasts and reprogrammed them. iPS has characteristics similar to embryonic stem cells (ES), but compared with ES which with limited source and ethical issues[15], iPS avoids the ethical restrictions of stem cell research and has abundant sources in accordance with relatively easy access. The advantages of individual-specific pluripotent stem cells have received wide public attention. Therefore, the emergence of iPS-Mφ provides a genotype-specific, scalable and reproducible source of human macrophages[11,16–22], it can also be genetically manipulated by CRISPR/Cas9-mediated gene editing and used in genetic engineering[23,24]. Compared with macrophages from other sources, iPS-Mφ are less difficult to operate, they have significant advantages over other cells and have been studied in many researches related to mechansims underlying diseases, especially the pathogenesis of immune diseases such as tuberculosis and tumors. For all these grounds, iPS-Mφ have broad application prospects.

To date, infectious disease like TB remains a very important public health issue worldwide, and Mycobacterium tuberculosis(Mtb) is known to be the main pathogen of TB [25]. Mtb belongs to intracellular parasites, tuberculosis can be simply understood as a series of continuous and slow interactions between Mtb and the immune system, which gives the body a sustained immune response. However, it is difficult for antibodies present in serum to enter the interior of the cells and kill Mtb. Therefore, the cellular immune response plays an important role in the body's resistance to Mtb infection. Current studies had found that the main host cell of Mtb is macrophage. When the infection begins, Mtb is engulfed by lung macrophages that have important immune effects against Mtb[26], when lung macrophages are infected with Mtb, they produce a series of immune responses to prevent the spread of them, and finally kill them. But Mtb can also survive in cells by evading the immune surveillance along with the attack of macrophages, and even lysing macrophages. Therefore, the interaction between Mφ and Mtb plays an important role in the study of the occurrence and development of tuberculosis.

The Bacillus Calmette-Guerin (BCG) is currently the only TB vaccine approved for marketing by the FDA. It was developed by two scientists: Guerin and Calmette, by culturing a poisonous Bovine M. tuberculosis into a vaccine-free attenuated strain. Since 1923, more than 4 billion people have been vaccinated by BCG worldwide [27]. But BCG has very little effect on adult TB and Mtb latent infection, more importantly, problems such as inability to be applied to immunodeficiency and prone to strain variation are also gradually exposed [28]. A variety of improved vaccines based on BCG, such as recombinant BCG, subunit vaccine, live vector vaccine, whole-cell inactivated vaccine and live attenuated vaccine, have been gradually developed due to these defects of BCG. Despite this, BCG is still favored by many scientists due to the low price and high safety as well as the efficiency in preventing TB infection in children.

Autophagy is a relatively conservative process in the evolution of organisms prevalent in eukaryotes[29] and an intracellular degradation pathway for damaged organelles and aggregation-prone proteins [30,31]. Through the process of autophagy, misfolded proteins, senescent organelles and invading pathogens are delivered to the lysosome by double-membrane vesicles for degradation to maintain cell homeostasis [32–35]. Autophagy is also an indispensable part of human health which is involved in a variety of diseases [36], including cancer [37], neurodegenerative diseases [38] and microbial infections [39,40]. Thereby, autophagy is a crucial cellular machinery conserved from yeast to higher eukaryotes that maintains organ metabolism, genome stability, and cell survival, and functions as either tumor suppressor at early stage or promotor at late stage[41]. Studies have confirmed that autophagy plays a unique role in the struggle between Mtb and Mφ. Mtb can activate autophagy after infection with Mφ, while autophagy is involved in the clearance of Mtb by Mφ[42]. Autophagy ubiquitin-like protein has been revealed to be involved in the promotion of anti-tuberculosis function in macrophages[42,43], the stimulation of autophagy in macrophages leads to the maturation of Mtb phagosomes into phagolysosomes, moreover, the induction of autophagy inhibits the survival of Mtb in macrophages. On the other hand, Mtb can escape the killing effect of autophagy [44–46], Mtb persists in macrophage phagocytosis by interfering with macrophage phagocytic lysosomal production, dysfunctional lysosomes are more susceptible to Mtb by inhibiting autophagy and directed migration of macrophages [47].

In conclusion, autophagy plays an important role in the involvement of macrophages in immune responses [48,49]. However, in the process of infection by Mtb, there are many factors remains unclear, for instance, the autophagy-related genes and proteome involved in the formation of autophagy and the signaling pathways involved in the entire autophagy process. Furthermore, when macrophages from different sources are infected with Mtb, the signaling pathways for activation or inhibition may differ. In our previous studies, we have successfully established macrophages derived from hiPS by using the EB differentiation method and macrophages derived from THP-1 by using PMA (PKC activator). Therefore, this study is aimed to investigate the differences and similarities of the role of autophagy and the mechanism underlying in Mtb-infected hiPS-Mφ and THP-1-Mφ. This will further elucidate the mechanism behind the action of macrophages in anti-tuberculosis immune response and lay the foundation for revealing the pathogenesis of Mtb infection.

2. Material And Methods

2.1 Cell culture

Human iPS cells (DYR0100) were cultured under feeder-free culture conditions in chemically defined mTeSR™1 medium (Stem Cell Technologies, Inc., Vancouver, BC, Canada) on matrigel-coated (Corning, Inc., NY, USA) dishes; and maintained in our laboratory in the Department of Biochemistry and Molecular Biology, College of Life Science and Medicine, Zhejiang Sci-Tech University (Hangzhou, ZJ, China). The cells were cultured in 5% CO_2 with 95% humidity at 37°C in mTeSR™1 medium, supplemented with 10μM Rho-associated kinase (ROCK) inhibitor Y27632 (Stem Cell Technologies, Inc., Vancouver, BC, Canada). The hiPS were passaged when they reached 80-90% con-fluency. For passage, the cells were incubated with Accutase™ (Stem Cell Technologies, Inc., Vancouver, BC, Canada) to a single-cell mass and replated on matrigel-coated dishes according to the appropriate split ratio. The medium was replaced daily. Human monocyte cell line THP-1 cells were provided by Dr. Caiyun Fu, Zhejiang Sci-Tech University and maintained in our laboratory in the Department of Biochemistry and Molecular Biology, College of Life Science and Medicine, Zhejiang Sci-Tech University (Hangzhou, ZJ, China). The THP-1 cells were cultured in 5% CO_2 with 95% humidity at 37°C in RPMI 1640 medium (Gibco, NY, USA), supplemented with 10% Fetal Bovine Serum (FBS, Gibco, NY, USA) and 1% Penicillin-Streptomycin (PSA, Gibco, NY, USA).

2.2 Macrophages differentiation from hiPS

hiPS-Mφ were generated by using a previously established protocol in our previous work[50]. The hiPS were gently digested with Accutase™ (StemCell Technologies, Inc., Vancouver, BC, Canada), and 2×10^6 cells were resuspended in Knockout-DMEM medium (KO-DMEM, Gibco, NY, USA) supplemented with 10% Knockout-serum replacement (KSR, Gibco, NY, USA), 1% Non-essential amino acids (NEAA, Gibco, NY, USA), 1 mM L-Glutamine (Sigma-Aldrich, St. Louis, MO, USA), 50 μM β-mercaptoethanol (β-ME, Solarbio, BJ, China) and 10 μM ROCK-inhibitor Y-27632 and then cultured on 6-well ultra-low attachment plates (Corning, SH, China) for 24 h. The medium was changed daily. After 8–11 days, EB were seeded onto gelatin-coated 24-well plates in DMEM medium (Gibco, NY, USA) supplemented with 10% FBS, 1 mM L-Glutamine, 50 μM β-ME, 50 ng/mL human macrophage colony-stimulating factor (M-CSF, PeproTech, Rocky Hill, NJ, USA), and 25ng/mL human IL-3 (Gibco, NY, USA) at a scale of 6–8 EB per well. The medium was changed every 3 days. Continuous monocyte production was cultured for 17–19 days. Non-adherent monocytes were collected every 4 days and other cells were continuously cultured, the adherent cells were further cultured for 2-3 weeks to collect suspended cells. Non-adherent monocytes were cultured in RPMI 1640 medium supplemented with 10% FBS, 100ng/mL M-CSF, 50 ng/mL interleukin (IL)-3, and 50 μM β-ME, and then used for identification experiments after 10 days.

2.3 Macrophages differentiation from THP-1

THP-1 cells were centrifuged at 1000 rpm for 5 min, the supernatant were discarded, and then THP-1 cells were resuspended in medium supplemented with 100 ng/mL PMA (Beyotime, SH, China) and incubated

for 24 hours in 5% CO_2 with 95% humidity at 37℃. After that, cells were cultured with the original medium and the medium was changed every two days.

2.4 Giemsa stain assay.

The slides were stained for 30 min with a working solution of Giemsa stain prepared from a commercially available stock solution (Beijing Solarbio Science & Technology Co., Ltd., BJ, China) according to recommendations of the manufacturer. The slides were then washed 2×1 min in ddH_2O and air dried, then detected with microscope.

2.5 Phagocytosis assay. The medium of hiPS-Mφ and THP-1-Mφ was aspirated, and then washed cells once with PBS. The Indian ink was diluted to the medium at a ratio of 1:1000 and mixed, the reagent was added to the cell culture dish and incubated in 5% CO_2 with 95% humidity at 37℃ for 1 h , and cells were observed under the microscope.

2.6 BCG infection

Fully dissolve BCG lyophilized powder with sterile physiological saline and the concentration of BCG strain after constant volume is 1×10^7 CFU/mL. hiPS-Mφ and THP-1-Mφ were infected with 10 MOI of BCG indicated condition priorto were harvested for analysis.

2.7 Preparation and analysis of transcriptome sequencing samples

After BCG-infected cells were cultured for 24 h, the cells were digested by 0.25% trypsin (Gibco, NY, USA) and harvested. The total RNA of the cells was extracted according to the Trizol product specification, and the purity and concentration of the RNA samples were determined by an Agilent 2100 Analyzer (USA). After the total RNA of the sample had passed the test, the sequencing library was established according to the standard procedure and was sequenced using Illumina Hiseq4000 with a sequencing read length of 150 bp (PE150). According to the standard transcriptome sequencing analysis process, sequencing data output statistics, gene expression level analysis, differential gene expression analysis, differential gene KEGG enrichment analysis and differential gene GO enrichment analysis were performed.

2.8 Scanning electron microscope

The sample was immersed in Gluta fixative at 4℃ overnight and then post-fixed for1-2 h in1% citric acid solution, dehydrated in ethanol. And the sample was dried using a Hitachi HCP-2 critical point dryer to reach the dry critical point. The above-prepared sample was observed by a scanning electron microscope (SU-8010 type, Hitachi), and photographed.

2.9 Transmission electron microscope

The sample was immersed in Gluta fixative at 4℃ overnight, post-fixed for 1-2 h in1% citric acid solution, dehydrated in ethanol and embedded with a mixture of Spurr embedding agent and acetone (V/V =

1/1).The sample was sliced using a LEICA EM UC7 ultrathin slicer with a thickness of 70-90 nm; the obtained sections were stained with lead citrate solution, uranyl acetate and 50% ethanol saturated solution for 5-10 min. Finally, the sections were observed and photographed in a transmission electron microscope (H-7650,Hitachi).

2.10 Real-time Quantitative PCR Detecting System (qPCR)

RNA was extracted by using TRIzol^{TM} Reagent, and cDNA was obtained by reverse transcription using the PrimeScript RT Reagent Kit according to the instructions. The qPCR analysis was set up in duplicate with SYBR Premix Ex Taq (Takara Bio, Inc., BJ, China) and performed using the 7500 Real-Time PCR system (Applied Biosystems; Thermo Fisher Scientific, Inc.). The cDNA was used as a template for qPCR, using β-actin as the internal reference gene, the relative expression of mRNA was calculated by $2^{-\Delta\Delta CT}$ method, and the results were statistically plotted. The mRNA fluorescent quantitative PCR primer information is shown in Table3. All primers were synthesized by Bio-Bioengineering Co., Ltd (Shanghai, China) .

2.11 Laser confocal detection of autophagy protein expression

The Ad-mCherry-GFP-LC3B was purchased from Beyotime (Shanghai, China) .The cells were seeded at 1 × 10^5 cells/well into 24-well plates. The Ad-mCherry-GFP-LC3Bwas added at an MOI of 20, and we observed the expression of fluorescent proteins after 24 h and 48 h of infection by laser scanning confocal microscope. Red puncta represented autolysosome, and yellow puncta overlaid by green and red appearing in the images indicated autophagosomes formation. they were counted to determine the autophagy level.

2.12 Western blot analysis

The cells were homogenized in lysis buffer (IP Buffer, 10 μg/μL Aprotinin,10 μg/μL Leupeptin, 100 mM PMSF,200 mM Vanadate (pH 10.0)overnight at 4℃, the lysates were centrifuged at 13,000 × g for 30 min at 4℃, and the supernatants were collected.The soluble protein concentration was determined via the Quick Start Bradford Protein Assay kit. And then the cell extracts (20 μg) were separated by 12% sodium dodecyl sulphate (SDS)-polyacrylamide gel electrophoresis and transferred toa nitrocellulose membrane (EMD Millipore). The membrane was blocked by 5% fat-free dry milk in PBS with 0.1% Tween-20 and probed by antibodies against LC3B (Abcam),GABARAPL2 (Abcam), Cathepsin D (Abcam), RAB7B (Abcam), DDIT4 (Abcam), EXOC8 (Novus), HRP-conjugated Affinipure Goat Anti-Rabbit IgG (H+L) (Proteintech), GAPDH(Proteintech), HRP-conjugated Affinipure Goat Anti-Mouse IgG (H+L) (Proteintech), mTOR (Cell signaling), p-mTOR (Cell signaling), Akt (Cell signaling), p-Akt (Cell signaling), Beclin1 (MBL BEIJING BIOTECH CO.,LTD) at a dilution of 1:1,000,followed by horseradish peroxidase (HRP)-conjugated secondary anti-rabbit IgG-HRP antibodiesor anti-mouse IgG-HRP antibodies (1:1,000, Beyotime, Shanghai, China).The blots were then developed using enhanced chemiluminescence (ECL) (Amersham; GE Healthcare Life Sciences, Piscataway, NJ, USA)or the ECL Tanon 5500 system (Tanon Science and Technology Co., Ltd., Shanghai, China).

2.13 Statistical analysis

Statistical analysis was conducted with GraphPad Prism 7 software. One-way ANOVA with uncorrected Fisher's least significant differences test was applied for the analysis of two independent variables. Comparison between two samples was done with the unpaired t test. More details are described in the figure legends. Mean values of three independent experiments are shown. Error bars are shown as mean ± SD. ns, non-significant,*p < 0.05, **p < 0.01, ***p < 0.001, ****p < 0.0001.

3. Results

3.1 Preparation and growth of functional macrophages derived from hiPS and THP-1.

To establish a hiPS-Mφ model, hiPS was induced to EB and matured after 8–11 days of culture. When EB was completely adherent, it began to differentiate toward monocytes. After culturing for about 12–20 days, suspended cells gradually appeared and were collected every 4–5 days into a new gelatin-coated petri dish and the remaining adherent cells continued to be cultured in fresh monocyte medium. Macrophage medium containing two cytokines of IL-3 and M-CSF at the same concentration was added to the collected suspension cells to differentiate monocytes into macrophages. The matured macrophages were observed to have typical macrophage morphology under the microscope (Figure.1A). Meanwhile, THP-1 cells were initially circular suspension cells, and were cultured in the original medium for several days after being treated with PMA for 24 hours. The cells were adherent and had various forms, such as ellipse, fusiform, irregular shape, etc., which conformed to the morphology of typical macrophages. The collected hiPS-Mφ and THP-1-Mφ with typical macrophage morphological characteristics were identified by Giemsa stain assay. After staining, the color of the cells changed to purple and the shape of the cells displayed round, oval, spindle-shaped and irregularly shaped. Some cells were observed as convex pseudopods with other typical Mφ morphological characteristics upon bright-field microscopy (Fig. 1B). The phagocytic ink granule level was determined by performing an ink phagocytosis test on the obtained macrophage-like cells. As a result, the macrophage-like cells had ink particles in the cytoplasm, indicating that they had a phagocytic function (Fig. 1C). All results further confirmed the establishment of the functionally active hiPS-Mφ and THP-1-Mφ model.

3.2 BCG induced autophagy in hiPS-Mφ and THP-1-Mφ

To verify whether BCG could induce autophagy in hiPS-Mφ and THP-1-Mφ, hiPS-Mφ, THP-1-Mφ, hiPS-Mφ infected with BCG and THP-1-Mφ infected with BCG were observed by scanning electron microscope (SEM) and transmission electron microscope (TEM). SEM observation showed that after 24 hours of BCG infection of hiPS-Mφ, the cells began to shrink and severe lysis occurred. The distribution of rod-shaped bacteria was observed in the extracellular cells (Fig. 2A). At the same time, similar changes occurred in THP-1-Mφ after 24 h of BCG infection (Fig. 2B). TEM observation showed that after 24 hours of BCG infection of hiPS-Mφ, the endoplasmic reticulum was swollen and the number of autophagosomes

increased, but it was not obvious (Fig. 3A). When BCG infected THP-1-Mφ cells for 24 h, the number of autophagosomes increased significantly, but the endoplasmic reticulum did not show obvious swelling like hiPS-Mφ (Fig. 3B).

To ascertain whether BCG would induce autophagy in hiPS-Mφ and THP-1-Mφ, hiPS-Mφ, hiPS-Mφ infected with BCG, THP-1-Mφ and THP-1-Mφ infected with BCG were transfected with Ad-mCherry-GFP-LC3B to monitor autophagic flux. In the case of non-autophagy, Ad-mCherry-GFP-LC3B will cause the cells to exhibit diffuse yellow fluorescence due to the superposition of mCherry and GFP. While in the case of autophagy, the GFP signal is unstable in the acidic conditions of the lysosome lumen and mCherry is acid-stable. Thus, colocalization of both GFP and mCherry fluorescence (yellow puncta) indicates that an autophagosome has not fused with a lysosome, whereas a mCherry signal without GFP (red puncta) indicates an autolysosome formation[51]. Laser confocal microscopy showed that after infecting with Ad-mCherry-GFP-LC3B for 24 h and 48 h, the inhibition or promotion of autophagy was more obvious after 48 h of infection than that of 24 h (Fig. 4, 5). Besides, we also studied the effect of the 3-methyladenine (3-MA) which is a class III PI3K inhibitor and can be used to inhibit autophagy, laser confocal microscopy showed that the fluorescence of the control cells and the 3-MA-treated hiPS-Mφ were weak and diffusely presented in the cytoplasm, indicating that the number of intracellular autophagosomes is small (Fig. 4, 5). The fluorescence of hiPS-Mφ and THP-1-Mφ in the BCG treatment group was mostly aggregated spots, and the fluorescence intensity was strong, indicating that the cells were autophagic, and the number of autophagosomes was high. At the same time, some cells had only red puncta, indicating the formation of autolysosomes and the cells were in the late stage of autophagy. Besides, the fluorescence expression of hiPS-Mφ and THP-1-Mφ in the 3-MA + BCG treatment group was similar to that in the BCG treatment group, except that the fluorescence intensity and the spots were slightly lower, indicating the degree of autophagy was slightly lower than that of the BCG treatment group(Fig. 4, 5).

3.3 BCG promotes hiPS-Mφ and THP-1-Mφ autophagy activation via regulating the expression of autophagy-related genes

Control hiPS-Mφ samples (Control_1, Control_2, and Control_3) and BCG-infected hiPS-Mφ samples (BCG _1, BCG _2, and BCG _3) were sent to Lianchuan Biotech (Hangzhou, China) for transcriptome sequencing and sequenced by HiSeq 4000 high-throughput sequencing. The original sequencing amount (Raw data), effective data (Clean data) and the proportion of bases with a mass value ≥ 30 (Q30) were sequenced. The results are shown in Table 1. According to the analysis, the proportion of valid data in the six samples was 97.88%, 97.94%, 98.14%, 97.96%, 97.93%, and 97.47% respectively, and Q30 was 97.33%, 97.39%, 97.41%, 97.19%, 97.44% and 97.37% respectively. According to the above data, the sequencing quality is excellent and the data can be further analyzed (Table 1). At the same time, Control THP-1-Mφ samples (Control_1, Control_2, and Control_3) and BCG-infected THP-1-Mφ samples (BCG _1, BCG _2, and BCG _3) were also sent to Lianchuan Biotech for same tests. The results are shown in Table 2. According to the analysis, the proportion of valid data in the six samples was 9 98.72%□98.73%□98.71%□98.81%□

98.80% and 98.37% respectively, and Q30 was 96.91%、97.00%、96.94%、97.36%、96.68% and 96.49% respectively. According to the above data, the data can be further analyzed (Table 2).

Table 1
Statistical analysis of sequencing data of hiPS-Mφ cells

sample name	Sequencing raw data	Sequencing valid data	Effective data ratio (%)	Q30(%)
Control_1	50670304	49598612	97.88	97.33
Control_2	44598474	43679992	97.94	97.39
Control_3	46519212	45652380	98.14	97.41
BCG_1	45306706	44382088	97.96	97.19
BCG_2	47506066	46521820	97.93	97.44
BCG_3	50879468	49594510	97.47	97.37

Table 2
Statistical analysis of sequencing data of THP-1-Mφ cells

sample name	Sequencing raw data	Sequencing valid data	Effective data ratio (%)	Q30(%)
Control_1	41129682	40602550	98.72	96.91
Control_2	43394438	42842628	98.73	97.00
Control_3	43106140	42550410	98.71	96.94
BCG_1	56922002	56243730	98.81	97.36
BCG_2	40588982	40100550	98.80	96.68
BCG_3	26601860	26168924	98.37	96.49

The abundance values of gene expression were measured using FPKM (Fragments Per Kilobase of exon model per Million mapped reads). FPKM represents the number of sequencing fragments contained in the bases per thousand transcripts sequenced per million sequencing bases. Briefly, the FPKM value can be understood as the amount of expression of a gene. Plotting the FPKM data of each sample into a box plot can intuitively understand the level of gene expression from the overall level, and for samples with biological replicates, it can also be used to initially judge the repeatability of the designed sample. In the figure, the abscissa is the name of the sample, and the ordinate is log10 (FPKM). The box plot of each region corresponds to five statistics (top to bottom, maximum, upper quartile, median, lower four quantile and minimum). It can be seen from the figure that the hiPS-Mφ and THP-1-Mφ has sample repeatability (Fig. 6A, B). The value of log10 (FPKM) of the different expression levels of different samples was plotted

as an expression density map, which can compare the changes in expression trends between different samples. In the figure, the abscissa is log10 (FPKM) and the ordinate is the density of the gene. It can be seen from Fig. 6A.b and Fig. 6B.b that the bio-repetition of hiPS-Mφ and THP-1-Mφ tends to be the same, but the expression trends of these two cells are different. Differential expression analysis was performed on all genes according to the significant difference threshold of |log2 (Fold Change, FC)| ≥1, $p < 0.05$ (where Fold change indicates the fold difference). The statistical results showed that compared with the control hiPS-Mφ, BCG-treated hiPS-Mφ had 832 significantly differentially expressed genes, of which 572 genes were up-regulated and 260 genes were down-regulated (Fig. 7A). Compared with the control THP-1-Mφ, BCG-treated THP-1-Mφ had 397 significant differentially expressed genes, of which 211 genes were up-regulated and 186 genes were down-regulated (Fig. 7B). As shown in the Fig. 7A.a and Fig. 7B.a, the volcano map can understand the overall distribution of differentially expressed genes. Therefore, the volcano map is further analyzed for the differential gene expression level. The volcano map uses log2 (Fold Change, FC) as the abscissa and -log10 (p-value) (represents the statistical significance of the difference in gene expression change) as the ordinate. All genes in the expression analysis were added for mapping. Among them, red represents a significantly differentially expressed gene that is up-regulated, blue represents a significantly differentially expressed gene that is down-regulated, and gray represents a non-significantly differentially expressed gene.

Differential gene cluster analysis can be used to determine the clustering pattern of genes under different experimental conditions. According to the similarity of the gene expression profiles of the samples, the genes were clustered and analyzed to visually show the expression of the genes in different samples, and then the biological related information was obtained. To better reflect the cluster expression pattern, log10 (FPKM + 1) was used for gene expression display, and the differential gene FPKM was displayed by Z value. The results are shown in Fig. 8, in which the abscissa is the sample name, the ordinate is the name of the differentially expressed gene, the different colors indicate different gene expression levels, and the color is expressed in blue from white to red to indicate the expression level from low to high. Red indicates a highly expressed gene and dark blue indicates a low expressed gene. The results showed that in the regulation of autophagy-related genes, DNA damage-inducible transcript 4 (*DDIT4*) and Exocyst complex component 8 (*EXOC8*) were significantly up-regulated in hiPS-Mφ. That means, the expression of *DDIT4* and *EXOC8* genes in hiPS-Mφ was significantly increased after BCG infection compared with the expression in uninfected cells ($P < 0.0001$) (Fig. 8A). At the same time, cathepsin D (*CTSD*) and *RAB7B* were significantly down-regulated in THP-1-Mφ, that means, compared with uninfected THP-1-Mφ cells, the expression of *CTSD* and *RAB7B* genes in THP-1-Mφ was significantly inhibited after BCG infection ($P < 0.0001$) (Fig. 8B). The GO enrichment analysis results histogram is a distribution of the number of differential genes reflected in the GO term enriched in the cellular component, the biological process, and the molecular function. The result is shown in Fig. 9A. In the hiPS-Mφ group, GO enrichment analysis of differentially expressed genes indicated that it is mainly involved in processes such as transcriptional regulation, signal transduction, cell membrane composition and protein binding. While in the THP-1-Mφ group, GO enrichment analysis of differentially expressed genes indicated that it is mainly involved in

signal transduction, inflammatory response, immune response, cell membrane composition and protein binding (Fig. 9B).

The Kyoto Encyclopedia of Genes and Genomes (KEGG) is a public database commonly used in genome deciphering. Genomic information is stored in a gene database, including intact and partially sequenced genomic sequences; more advanced functions are stored in the Pathway database, including graphical cell biochemical processes such as metabolism, membrane transport, signaling, and cell cycle. Therefore, the analysis of the pathway will help us better understand the biological functions of genes. KEGG is an important public database on Pathway that provides integrated pathway queries that provide not only all possible metabolic pathways, but also comprehensive and detailed annotation of the enzymes involved in the catalysis of each step. The KEGG enrichment analysis was performed using ggplot2, and the analysis results were plotted as scatter plots. The Rich Factor in the figure indicates the number of differential genes located in the KEGG / the total number of genes in the KEGG, the larger the enrichment factor value, the greater the degree of KEGG enrichment. Figure 10A shows a partial integrative metabolic pathway for KEGG enrichment analysis of hiPS-Mφ after BCG treatment. It can be seen that the pathway associated with inflammation, autophagy, apoptosis, etc. changes siginificantly in hiPS-Mφ treated with BCG. At the same time, Fig. 10B shows a partial integrative metabolic pathway for KEGG enrichment analysis of THP-1-Mφ after BCG treatment. It can be seen from the figure that pathway associated with inflammation, autophagy, apoptosis, etc. also changes siginificantly in THP-1-Mφ after BCG treatment. Compared with THP-1-Mφ, hiPS-Mφ is enriched in tuberculosis, Toll-like receptors, TNF, PI3K-AKT, phagosomes, nodular receptors, NF-κB, mTOR, MAPK, IL-17, chemokine signaling pathway, autophagy pathway and apoptotic pathways, but the enrichment factors are different, indicating the number of differential genes is different. Based on this, it is speculated that there are some differences in the mechanism underlying anti-tuberculosis immunity in hiPS-Mφ and THP-1-Mφ after BCG infection.

The expression levels of autophagy-related genes *LC3B*, *GABARAPL2*, *P62*, *DDIT4*, *EXOC8*, *CTSD* and *RAB7B* were detected by qPCR after extracting total RNA of hiPS-Mφ with BCG infection. In general, when autophagy is promoted, *LC3B* rises, *GABARAPL2* decreases, and *P62* decreases. Conversely, when autophagy is suppressed, *LC3B* decreases, *GABARAPL2* rises, and *P62* rises. Compared with uninfected hiPS-Mφ, the expression of *LC3B* was significantly increased in hiPS-Mφ after BCG infection($P < 0.0001$), the expression of *GABARAPL2* was significantly decreased ($P < 0.0001$), and the expression of *P62* was significantly decreased ($P < 0.01$) (Fig. 11A). Based on this, it is possible that the occurrence of autophagy was promoted by regulating the expression of the above genes in hiPS-Mφ with BCG infection. At the same time, the autophagy-related genes *DDIT4* and *EXOC8* genes are also significantly up-regulated in transcriptome sequencing, indicating that qPCR verification results are consistent with hiPS-Mφ sequencing results. Similarly, the expression of *LC3B* gene was significantly increased after BCG infection of THP-1-Mφ ($P < 0.05$), the expression of *GABARAPL2* gene was significantly decreased ($P < 0.001$), and the expression of *P62* gene was significantly decreased($P < 0.01$). It can be speculated that the occurrence of autophagy was promoted by regulating the expression of *CTSD* and *RAB7B* in THP-1-Mφ with BCG infection. At the same time, *CTSD* and *RAB7B* are the significant down-regulated autophagy-

related genes found in the THP-1-Mφ transcriptome sequencing. The qPCR verification results are consistent with the sequencing results (Fig. 11B).

3.4 PI3K-AKT-mTOR pathway is involved in hiPS-Mφ and THP-1-Mφ in response to tuberculosis infection

The total protein of hiPS-Mφ and THP-1-Mφ treated in the control group, 3-MA group, BCG group and 3-MA + BCG group were extracted. Western Blot Analysis was used to detect the changes in the expression of autophagy-related proteins such as LC3B, GABARAPL2, Beclin1 and the expression of proteins involved in in PI3K-AKT-mTOR signaling pathway. The expression of DDIT4 and EXOC8 in the hiPS-Mφ group along with the expression of RAB7B and CTSD in the THP-1-Mφ group was detected in accordance with the results of transcriptome sequencing analysis. As can be seen from the Fig. 12, the expression of GABARAPL2, p-AKT and Beclin1 in the hiPS-Mφ treated with BCG was significantly lower than that of the control group($P < 0.0001$), and the expreesion of p-mTOR decreased slightly ($P < 0.05$). When it comes to THP-1-Mφ, the expression of GABARARL2, p-mTOR and p-AKT in the THP-1-Mφ treated with BCG was significantly lower than that of the control group($P < 0.01$), and the expression of Beclin1 increased slightly ($P < 0.05$). The ratio of *LC3BII/I* in the hiPS-Mφ and THP-1-Mφ treated with BCG increased significantly ($P < 0.0001$). The results of the 3-MA treatment group were almost reversed, it was demonstrated that 3-MA treatment inhibited autophagy, while BCG infection promoted autophagy. Autophagy also occurred in the 3-MA + BCG group, but the autophagy in the BCG group was more pronounced. In addition, the expression of DDIT4 and EXOC8 was increased in hiPS-Mφ treated with BCG ($P < 0.0001$), and the expression of RAB7B and CTSD was decreased in THP-1-Mφ after treatment with BCG ($P < 0.001$). The results of the transcript level test are consistent with the results of the protein level test. Besides, when hiPS-Mφ were treated with 3-MA, the expression levels of *DDIT4* and *EXOC8* decreased when autophagy was inhibited ($P < 0.001$) and when THP-1-Mφ were treated with 3-MA, the expression of *RAB7B* and *CTSD* increased when autophagy was inhibited. ($P < 0.0001$).

In conclusion, this study showed that after BCG infection, the autophagy morphology and expression of autophagy-related genes in hiPS-Mφ and THP-1-Mφ cells changed significantly. It is preliminarily speculated that the expression of autophagy-related genes is regulated by PI3K/AKT/mTOR signaling pathway after BCG infection to promote the occurrence of autophagy. The difference is that for hiPS-Mφ cells, *DDIT4* and *EXOC8* genes are regulating the occurrence of autophagy, that is, the expression level increases when autophagy occurs, and for THP-1-Mφ, the *RAB7B* and *CTSD* genes negatively regulate the occurrence of autophagy, that is, the expression level decreases when autophagy occurs. The differences in the expression of genes and proteomes caused by BCG-induced autophagy in macrophages derived from different sources and their specific regulatory mechanisms need further investigation.
Table 3: The primer used in this study

Gene	Forward primer(5'-3') a	Reverse primer(5'-3')
β-actin	AGCGAGCATCCCCCAAAGTT	GGGCACGAAGGCTCATCATT
LC3B	TTCGAGAGCAGCATCCAACC	AGATTGGTGTGGAGACGCTGA
GABARAPL2	GAAGTGGATGTTCAAGGAGGAC	ATAGTTAGGCTGGACTGTGGGA
P62	CTGCTGCTCTTCTGCCTGTGC	AGGAACTCCCGCTGGTAAACG
RAB7B	GTGGACCTGAAACTCATTATCGT	CAGTGTGGTCTGGTATTCCTCAT
CTSD	CCGAGGTGCTCAAGAACTACAT	AGGCTGACGACGCTGACTG
DDIT4	CTCGTCCTTGCCCCGAACTCCCA	CGAAGCCACTGTTGCTGCTGTCC
EXOC8	GAAGCCACTAAACATCGCAACTC	TTACTTACCCCACAACTTTTCATCT

4. Discussion

The macrophages currently used for immune responses are tumor cell lines-derived macrophages and primary cell lines-derived macrophages, but such cells have many disadvantages. The karyotype and function of macrophages derived from tumor cell lines (such as U937,THP-1) are easy to be abnormal. Primary cells are difficult to be genetically manipulated because of the individual differences and low availablity, furthermore,they cannot be self-renewing. To solve all these problems, stem cells become an effective and practical source of macrophages. Macrophages derived from hES and hiPS are most commonly used in related researches but hES-Mφ have ethical problems, the selection of hiPS-Mφ as a research object can overcome the above-mentioned deficiencies. In addition, hiPS-derived monocytes and macrophages could potentially be a useful source of patient-specific cells that are difficult or impossible to derive[52]. We have established the protocol to obtain macrophage derived from hiPS by using EB induced differentiation method. At the same time, THP-1-Mφ were obtained for comparison. We have performed a series of related identification tests on the hiPS-Mφ and THP-1-Mφ to determine whether we really get functional hiPS-Mφ and THP-1-Mφ. The main methods in our research include ink phagocytosis detection and Gimesa staining. As a result, it was confirmed that hiPS-Mφ and THP-1- Mφ can be dyed purple by the Giemsa Stain solution, and can also engulf ink particles. Based on the above experimental results, it can be determined that we have successfully obtained functionally active macrophages induced by hiPS and THP-1.

In addition, hiPS-Mφ and THP-1-Mφ was infected with BCG in this research and then subjected to transcriptome sequencing analysis, and the KEGG enrichment of BCG-infected hiPS-Mφ and THP-1-Mφ was further analyzed. The integrated metabolic pathway involved inflammation, apoptosis, self-induction

and autophagy, etc., and is enriched in these aspects. Among them, in autophagy pathway, BCG infected hiPS-Mφ was significantly up-regulated by *DDIT4* and *EXOC*8 genes ($P < 0.0001$). DDIT4 [53,54] is present in the cytoplasm and is induced to be highly expressed under various adverse conditions such as hypoxia, insufficient nutrient supply, and oxidative stress. *DDIT*4 can promote autophagy of cells by inhibiting the target of mTOR kinase complex 1 (mTORC1) and regulating Atg4B activity. Exocyst Complex 8 (EXOC8) is one of the eight subunits of the exocyst complex[55,56]. The main role of the exocyst complex lies in the regulation of cell polarity, the targeted transport of vesicles, and the migration of cells. Studies have shown that the function of exocyst complex is regulated by small GTPase, mammalian *EXOC8* is an effector of Ral GTPases, and Ral GTPases interact with *EXOC8* and another subunit Sec5 of exocyst complex to regulate the composition of exocyst[57–59]. The results of our research suggest that *DDIT4* and *EXOC8* may be involved in the Bacillus Calmette-Guerin induced autophagy. At the same time, the *CTSD* and *RAB7B* genes were significantly down-regulated in BCG-infected THP-1-Mφ ($P < 0.001$). It is suggested that there is a difference in BCG infection between hiPS-Mφ and THP-1-Mφ in the autophagy signaling pathway. *RAB7B* belongs to the small GTPase, Studies have shown that *RAB7B* regulates LC3 processing by interacting with Atg4B[60,61]. And *RAB7B* can negatively regulate lipopolysaccharide-treated macrophages, induce the production of TNF-α, IL-6, NO, and IFN-β, and enhance lipopolysaccharide-induced activation of mitogen-activated protein kinase, NF-κB and IFN. Regulating the Factor 3 signaling pathway, in turn, promotes degradation of TLR4. The Toll-like signaling pathway was activated in our transcriptome results[34], but there was no significant change in the expression of TLR4. It is speculated that THP-1-Mφ of BCG infection differs in innate immunity and autophagy. *CTSD* belongs to the endopeptidase, which is present in lysosomes and degrades peptides and proteins. It is involved in the regulation of physiological processes, such as the digestion of intracellular proteins, the activation of growth factors, peptides and hormones, the activation and processing of zymogens, the presentation of brain antigens and the programmed cell death[62]. Studies have found that when autophagy flux increases, lysosomes may be damaged and *CTSD* expression is inhibited[63]. Thus, in autophagy pathway, although the genes changed significantly after BCG infection of hiPS-Mφ and THP-1-Mφ were different, the signaling pathways involved are interrelated.

After BCG infection of macrophages, an increase in autophagosomes was also observed from the submicroscopic structure. Besides, the study also found that autophagy has a highly evolved nature, its occurrence and development are regulated by a variety of autophagy-related genes. At present, at least 30 autophagy-specific genes and more than 50 related genes have been identified[64]. *LC3B, GABARAP* and *P62* are typical autophagy markers [65,66]. This study found that the expression of *LC3B* gene in BCG-infected hiPS-Mφ and BCG-infected THP-1-Mφ was increased ($P < 0.0001$), the expression of *GABARAPL2* and *P62* genes was decreased ($P < 0.01$). Then the BCG-infected hiPS-Mφ and BCG-infected THP-1-Mφ was treated with 3-methyladenine (3-MA). 3-MA is a popular inhibitor of the autophagic pathway and has been reported to inhibit the activity of PI3-Kinase. It can block the formation of preautophagosome, autophagosome and autophagic vacuoles[67]. Researches have reported that in the human myeloid leukemia cell line, K562, crotoxin-induced apoptotic cell death was potentiated by 3-MA[68]. And 3-MA also has been

reported as the contribution to the upregulation of oridonin-induced apoptosis in the human cervical carcinoma cell line, HeLa[69]. According to current researches, 3-MA or suppression of autophagy regulatory pathways may provoke apoptotic efficiency of chemotherapeutic agents in prostate[70], breast [71], colon[72], lung[73], HeLa cancer cells[69] and so on. From all these grounds, 3-MA can be defined as a suitable inhibitor of the autophagic pathway and can be used in our research as a contrast to BCG. According to the results, the expression level of the autophagy-related genes changed correspondingly, and the level of autophagy was also decreased after treated with 3-MA. At the same time, laser confocal detection of mCherry-GFP-LC3B fluorescent protein expression also confirmed that when BCG infected hiPS-Mφ and THP-1-Mφ, the fluorescence intensity and the number of autophagosomes increased, while the 3-MA + BCG group had weaker fluorescence than that of the BCG group. It was shown that 3-MA can inhibit autophagy caused by BCG infection and the mechanism may be related to the inhibition of 3-MA on PI3K as 3-MA is a class III PI3K inhibitor. A large amount of data indicates that autophagy is closely related to the PI3K/AKT/mTOR signaling pathway and the expression of DDIT4 is related to the PI3K/AKT pathway[74,75]. In this study, the above autophagy-related proteomes were detected. The results showed that the LC3BII/I ratio was significantly increased after BCG infection of hiPS-Mφ and THP-1-Mφ ($P < 0.0001$), and the expression of p-AKT decreased siginificantly ($P < 0.0001$). The expression of p-mTOR in hiPS-Mφ and THP-1-Mφ decreased after BCG infection, the difference is that it was signigicantly in THP-1-Mφ ($P < 0.0001$) but slightly in hiPS-Mφ ($P < 0.05$). The ratio of LC3BII/LC3BI was significantly decreased after 3-MA treatment of hiPS-Mφ and THP-1-Mφ ($P < 0.01$), and the expression of p-mTOR increased significantly ($P < 0.01$). The expression of p-AKT in hiPS-Mφ and THP-1-Mφ increased after 3-MA treatment, it was signigicantly in THP-1-Mφ ($P < 0.0001$) but only saw a small rise in hiPS-Mφ. All above results indicate that autophagy occurs in hiPS-Mφ and THP-1-Mφ, because post-translational modification of LC3 occurs during autophagy, lipiding LC3-I to LC3-II,LC3II is then modified at the C-terminus by phosphatidylethanolamine and tightly bound to the autophagosome membrane. In addition, in the transcriptome analysis, compared with the uninfected control cells, the expression of autophagy-related genes *DDIT4*, *EXOC8*, *RAB7B* and *CTSD* in the hiPS-Mφ and THP-1- Mφ after BCG infection was significantly different ($P < 0.0001$). Therefore, this experiment performs validation analysis at the mRNA and proteome levels. It was found that the expression of *DDIT4* and *EXOC8* genes was significantly increased when hiPS-Mφ was infected with BCG ($P < 0.0001$). When the inhibition of autophagy occurred, the expression levels of *DDIT4* and *EXOC8* genes decreased ($P < 0.0001$). At the same time, after BCG infection of THP-1-Mφ, the expression of *RAB7B* and *CTSD* gene decreased when autophagy was promoted ($P < 0.001$). When treated with 3-MA, the expression of *RAB7B* and *CTSD* increased when autophagy was inhibited. ($P < 0.001$).

The macrophages currently used in related research on immune diseases are mainly derived from tumor cell lines and primary cell lines which have many defects and limiations. Under these circumstances, hiPS-Mφ with a large number of advantages are very eager to be studied. However, based on the above results, there are some differences and relevances in the mechanisms involved in the occurrence of autophagy induced by BCG in macrophages derived from different sources (hiPS-Mφ and THP-1-Mφ). In order to find the pathogenesis and therapeutic targets of TB, establishing an *in vitro* TB model of hiPS-

Mφ is critical. While regarding the autophagy induced by BCG infection in macrophages derived from different sources, there are still some issues needed to be further clarified. For example, when BCG infection induces autophagy in hiPS-Mφ and THP-1-Mφ, the expression of some genes and proteomes is different, and the autophagy-related genes involved are also different, the reasons still remain unclear. Furthermore, the specific regulatory mechanisms involved and the differences of the mechanisms are still unclear and need further investigation. Before using hiPS-Mφ for TB pathogenesis and autophagy-related researches, a large variety of researches still urgently needed to be completed.

5. Conclusion

This study showed that after BCG infection, the autophagy morphology and expression of autophagy-related genes and proteomes in hiPS-Mφ and THP-1-Mφ changed significantly, and it is preliminarily speculated that the expression of autophagy-related genes is regulated by PI3K/AKT/mTOR signaling pathway after BCG infection to promote the occurrence of autophagy. The difference is that for hiPS-Mφ, *DDIT4* and *EXOC8* genes are positively regulating the occurrence of autophagy, and for THP-1-Mφ, the *RAB7B* and *CTSD* genes negatively regulate the occurrence of autophagy (Fig. 13).

Declarations

Acknowledgements

We would like to thank Stem Cell Bank, Chinese Academy of Sciences for kindly providing human iPS. We would like to thank Dr. Caiyun Fu, Zhejiang Sci-Tech University for kindly providing human monocyte cells (THP-1). We would like to thank Faculty of Agriculture, Life and Environmental Sciences, Zhejiang University for their technique support in detection of autophagy by Scanning electron microscope and Transmission electron microscope. We would like to thank Dr. Yulong He for assistance in the designing of the experiments.

Funding

This work was supported by grants from the Zhejiang Province Natural Science Foundation (Nos. LY17C120001). The funders had no role in study design, data collection and analysis, decision to publish, or preparation of the manuscript.

Ethics approval and consent to participate

Not applicable

Availability of data and materials

Not applicable

Authors' contributions

MZ , DH and OL are equally to this work. MZ , DH and OL participated in the experiments of human iPS differentiation and cell culture, MZ, DH, OL, AS, YL and WBO participated in the experiments of molecular biology. MZ, DH, OL and YW contributed to data analysis and manuscript writing. YW conceived the idea, designed the experiments, and provided administrative support and final approval of manuscript. All authors read and approved the final manuscript.

Disclosure of potential conflicts of interest

All authors declare that their participation in the study did not involve factual or potential conflicts of interests.

Consent for publication

Not applicable.

References

1. Boniakowski AE, Kimball AS, Jacobs BN, Kunkel SL, Gallagher KA. Macrophage-Mediated Inflammation in Normal and Diabetic Wound Healing. J Immunol. 2017;199:(17).
2. Gordon S, Martinez-Pomares L. Physiological roles of macrophages. Pflügers Archiv - European Journal of Physiology. 2017;469:(1–10).
3. Zhang M, et al. The MTOR Signaling Pathway Regulates Macrophage Differentiation from Mouse Myeloid Progenitors by Inhibiting Autophagy. *Autophagy* 2019.
4. Jiang Y, Zhao Y, Zhu X, Liu Y, Zhang X. Effects of autophagy on macrophage adhesion and migration in diabetic nephropathy. Ren Fail. 2019;41:(682–90).
5. Li W, et al. Macrophages are involved in the protective role of human umbilical cord-derived stromal cells in renal ischemia-reperfusion injury. Stem cell research. 2013;10:405–16. doi:10.1016/j.scr.2013.01.005.
6. Bolhuis RLH, Sturm E, Braakman E. T cell targeting in cancer therapy. Cancer Immunology Immunotherapy. 1991;34:(1–8).
7. Coussens LM, Laurence Z, Karolina A. P. Neutralizing tumor-promoting chronic inflammation: a magic bullet? Science. 2013;339:(286–291).
8. De Palma M, Lewis CE. Macrophage regulation of tumor responses to anticancer therapies. Cancer cell. 2013;23:277–86. doi:10.1016/j.ccr.2013.02.013.
9. Lewis CE, Pollard JW. Distinct role of macrophages in different tumor microenvironments. Cancer research. 2006;66:605–12. doi:10.1158/0008-5472.can-05-4005.
10. Cole T, et al. Differential gene and transcript expression analysis of RNA-seq experiments with TopHat and Cufflinks. NATURE PROTOCOLS. 2012;7:(562–578).
11. Zhaolei Z, et al. PseudoPipe: an automated pseudogene identification pipeline. Bioinformatics. 2006;22:(1437–1439).

12. Tsuchiya S, Yamabe M, Yamaguchi Y, Kobayashi Y, Tada K. Establishment and characterization of a human acute monocytic leukemia line (THP-1). Int J Cancer. 1980;26:(171–6).
13. Cousins RJ, Blanchard RK, Popp MP, Liu L, Green CL. A global view of the selectivity of zinc deprivation and excess on genes expressed in human THP-1 mononuclear cells. Proc Natl Acad Sci USA. 2003;100:(6952–6957).
14. Rogers PD, et al. Pneumolysin-dependent and -independent gene expression identified by cDNA microarray analysis of THP-1 human mononuclear cells stimulated by Streptococcus pneumoniae. Infect Immun. 2003;71:2087–94. doi:10.1128/iai.71.4.2087-2094.2003.
15. Evans MJ, Kaufman MH. Establishment in culture of pluripotential cells from mouse embryos. Nature. 1981;292:154–6. doi:10.1038/292154a0.
16. Hong D, et al. Human-induced pluripotent stem cell-derived macrophages and their immunological function in response to tuberculosis infection. Stem Cell Res Ther. 2018;9:(49).
17. Kaufman DS, Hanson ET, Lewis RL, Auerbach R, Thomson JA. Hematopoietic colony-forming cells derived from human embryonic stem cells. Proc Natl Acad Sci USA 2001, 98, (10716–10721), doi:10.1073/pnas.191362598.
18. Senju S, et al. Generation of dendritic cells and macrophages from human induced pluripotent stem cells aiming at cell therapy. Gene therapy. 2011;18:874–83. doi:10.1038/gt.2011.22.
19. Van WB, Cathy B, Jane V, A., C. S. & Tadeu CD, Efficient, Long Term Production of Monocyte-Derived Macrophages from Human Pluripotent Stem Cells under Partly-Defined and Fully-Defined Conditions. *Plos One* 2013, *8*, (e71098).
20. Yanagimachi MD, et al. Robust and Highly-Efficient Differentiation of Functional Monocytic Cells from Human Pluripotent Stem Cells under Serum- and Feeder Cell-Free Conditions. *Plos One* 2013, *8*, (e59243).
21. Zhan X, et al. Functional antigen-presenting leucocytes derived from human embryonic stem cells in vitro. Lancet. 2004;364:163–71. doi:10.1016/s0140-6736(04)16629-4.
22. Zhang H, et al. Functional analysis and transcriptomic profiling of iPSC-derived macrophages and their application in modeling Mendelian disease. Circulation research. 2015;117:17–28. doi:10.1161/circresaha.117.305860.
23. Gupta RM, Meissner TB, Cowan CA, Musunuru K. Genome-Edited Human Pluripotent Stem Cell-Derived Macrophages as a Model of Reverse Cholesterol Transport. Arterioscler Thromb Vasc Biol. 2016;36:(15–8).
24. Yeung ATY, et al. Exploiting induced pluripotent stem cell-derived macrophages to unravel host factors influencing Chlamydia trachomatis pathogenesis. Nat Commun. 2017;8:(15013).
25. Rangaka MX, et al. Controlling the seedbeds of tuberculosis: diagnosis and treatment of tuberculosis infection. Lancet. 2015;386:2344–53. doi:10.1016/s0140-6736(15)00323-2.
26. Cruz A, et al. IL-17A Promotes Intracellular Growth of Mycobacterium by Inhibiting Apoptosis of Infected Macrophages. *Front Immunol* 2015, *6*, (498).

27. Neha D, Ramsay AJ. Prime-boost approaches to tuberculosis vaccine development. Expert Review of Vaccines. 2012;11:(1221–1233).
28. Colditz GA, et al. Efficacy of BCG vaccine in the prevention of tuberculosis. Meta-analysis of the published literature. Jama the Journal of the American Medical Association. 1994;271:(698–702).
29. Qiu P, Liu Y, Zhang J. Review: the Role and Mechanisms of Macrophage Autophagy in Sepsis. Inflammation. 2019;42:(6–19).
30. Maetzel D, et al. Genetic and Chemical Correction of Cholesterol Accumulation and Impaired Autophagy in Hepatic and Neural Cells Derived from Niemann-Pick Type C Patient-Specific iPS Cells. Stem Cell Reports. 2014;2:(866–80).
31. Sangani R, et al. The crucial role of vitamin C and its transporter (SVCT2) in bone marrow stromal cell autophagy and apoptosis. Stem cell research. 2015;15:312–21. doi:10.1016/j.scr.2015.06.002.
32. Ong SB, et al. Calpain Inhibition Restores Autophagy and Prevents Mitochondrial Fragmentation in a Human iPSC Model of Diabetic Endotheliopathy. *Stem Cell Reports*.
33. Yang Z, Klionsky DJ. Eaten alive: a history of macroautophagy. Nat Cell Biol. 2010;12:(814).
34. Wu J, Deng X, Gao J, Gao W, Zhang Y Autophagy mediates the secretion of macrophage migration inhibitory factor from cardiomyocytes upon serum-starvation. *Science China. Life sciences* 2019.
35. 10.1371/journal.ppat.1002416
Besteiro S, Brooks CF, Striepen B, Dubremetz JF Autophagy protein Atg3 is essential for maintaining mitochondrial integrity and for normal intracellular development of Toxoplasma gondii tachyzoites. *PLoS Pathog* 2011, *7*, (e1002416), doi:10.1371/journal.ppat.1002416.
36. Schneider JL, Cuervo AM. Autophagy and human disease: emerging themes. Curr Opin Genet Dev. 2014;26:(16–23).
37. Onorati AV, Dyczynski M, Ojha R, Amaravadi RK Targeting autophagy in cancer. *Cancer* 2018, *124*.
38. Sahab UM, et al. Autophagy and Alzheimer's Disease: From Molecular Mechanisms to Therapeutic Implications. Frontiers in Aging Neuroscience. 2018;10:(1–18).
39. María LdA, Celina A, María C Rab GTPases and the Autophagy Pathway: Bacterial Targets for a Suitable Biogenesis and Trafficking of Their Own Vacuoles. *Cells* 2016, *5*, (11).
40. Saitoh T, Akira S. Regulation of inflammasomes by autophagy. J Allergy Clin Immunol. 2016;138: (28–36).
41. 10.1371/journal.ppat.1007541
Wang L, et al. p62-mediated Selective autophagy endows virus-transformed cells with insusceptibility to DNA damage under oxidative stress. *PLoS Pathog* 2019, *15*, (e1007541), doi:10.1371/journal.ppat.1007541.
42. Gutierrez MG, et al. Autophagy Is a Defense Mechanism Inhibiting BCG and Mycobacterium tuberculosis Survival in Infected Macrophages. Cell. 2004;119:(753–66).
43. Sakowski ET, Koster S, Celhay CP, Park HS, Philips JA Ubiquilin 1 Promotes IFN-γ-Induced Xenophagy of Mycobacterium tuberculosis. *Plos Pathogens* 2015, *11*, (e1005076).

44. Kusner DJ. Mechanisms of mycobacterial persistence in tuberculosis. Clinical Immunology. 2005;114:(239–247).
45. Landes MB, Rajaram MVS, Nguyen H, Schlesinger LS. Role for NOD2 in Mycobacterium tuberculosis-induced iNOS expression and NO production in human macrophages. J Leukoc Biol. 2015;97:(1111).
46. Vergne I, et al. Autophagy in Immune Defense Against Mcobacterium tuberculosis. Autophagy. 2006;2:(175–178).
47. Berg RD, et al. Lysosomal Disorders Drive Susceptibility to Tuberculosis by Compromising Macrophage Migration. Cell. 2016;165:(139–52).
48. Deretic V, et al. Immunologic manifestations of autophagy. Journal of Clinical Investigation. 2015;125:(75–84).
49. Deretic V, Levine B, Autophagy. Immunity, and Microbial Adaptations. Cell Host Microbe. 2009;5: (527–549).
50. Hong D, et al. Human-induced pluripotent stem cell-derived macrophages and their immunological function in response to tuberculosis infection. Stem Cell Res Ther 2018, 9, (49), doi:10.1186/s13287-018-0800-x.
51. Abuelezz SA. Nebivolol attenuates oxidative stress and inflammation in a guinea pig model of ovalbumin-induced asthma: a possible mechanism for its favorable respiratory effects. Can J Physiol Pharmacol. 2018;96:258–65. doi:10.1139/cjpp-2017-0230.
52. Cao X, et al. Differentiation and Functional Comparison of Monocytes and Macrophages from hiPSCs with Peripheral Blood Derivatives. Stem Cell Reports. 2019;12:1282–97. doi:10.1016/j.stemcr.2019.05.003.
53. Qiao S, et al. A REDD1/TXNIP pro-oxidant complex regulates ATG4B activity to control stress-induced autophagy and sustain exercise capacity. *Nature Communications* 2015, *6*, (7014).
54. Tan CY, Thilo H & G., H. T. mTORC1 Dependent Regulation of REDD1 Protein Stability. *Plos One* 2013, *8*, (e63970).
55. TerBush DR, Maurice T, Roth D, Novick P. The Exocyst is a multiprotein complex required for exocytosis in Saccharomyces cerevisiae. Embo Journal. 1996;15:(6483–94).
56. Hsu SC, et al. The mammalian brain rsec6/8 complex. Neuron. 1996;17:(1209–1219).
57. He B, Guo W. The exocyst complex in polarized exocytosis. Curr Opin Cell Biol. 2009;21:(537–542).
58. Moskalenko S, et al. Ral GTPases Regulate Exocyst Assembly through Dual Subunit Interactions. J Biol Chem. 2003;278:(51743–51748).
59. Wu H, Rossi G, Brennwald P. The ghost in the machine: small GTPases as spatial regulators of exocytosis. Trends Cell Biol. 2008;18:(397–404).
60. Kjos I, et al. Rab7b modulates autophagic flux by interacting with Atg4B. *EMBO reports*, (e201744069).
61. Wang Y, et al. Lysosome-associated small Rab GTPase Rab7b negatively regulates TLR4 signaling in macrophages by promoting lysosomal degradation of TLR4. 2007, *110*, (962–971).

62. Piwnica D, et al. Cathepsin D Processes Human Prolactin into Multiple 16K-Like N-Terminal Fragments: Study of Their Antiangiogenic Properties and Physiological Relevance. *Molecular Endocrinology*, *18*, (2522–2542).
63. L T, et al. Decreased expression of cathepsin D in monocytes is related to the defective degradation of amyloid-β in Alzheimer's disease. 2014, *42*, (511–520).
64. Geng J, Baba M, Nair U, Klionsky DJ. Quantitative analysis of autophagy-related protein stoichiometry by fluorescence microscopy. J Cell Biol. 2008;183:(1175–5).
65. Kabeya. & Y. LC3, GABARAP and GATE16 localize to autophagosomal membrane depending on form-II formation. J Cell Sci. 2004;117:(2805–12).
66. Wu J, Dang Y, Su W, Liu C, Yu L. Molecular cloning and characterization of rat LC3A and LC3B - Two novel markers of autophagosome. Biochemical Biophysical Research Communications. 2016;339:(437–442).
67. Petiot A, Ogier-Denis E, Blommaart EF, Meijer AJ, Codogno P. Distinct classes of phosphatidylinositol 3'-kinases are involved in signaling pathways that control macroautophagy in HT-29 cells. J Biol Chem. 2000;275:992–8. doi:10.1074/jbc.275.2.992.
68. Yan CH, et al. Contributions of autophagic and apoptotic mechanisms to CrTX-induced death of K562 cells. Toxicon: official journal of the International Society on Toxinology. 2006;47:521–30. doi:10.1016/j.toxicon.2006.01.010.
69. Cui Q, Tashiro S, Onodera S, Ikejima T. Augmentation of oridonin-induced apoptosis observed with reduced autophagy. J Pharmacol Sci. 2006;101:230–9. doi:10.1254/jphs.fpj06003x.
70. Kumar D, Shankar S, Srivastava RK. Rottlerin induces autophagy and apoptosis in prostate cancer stem cells via PI3K/Akt/mTOR signaling pathway. Cancer letters. 2014;343:179–89. doi:10.1016/j.canlet.2013.10.003.
71. Cui Q, Tashiro S, Onodera S, Minami M, Ikejima T. Autophagy preceded apoptosis in oridonin-treated human breast cancer MCF-7 cells. Biol Pharm Bull. 2007;30:859–64. doi:10.1248/bpb.30.859.
72. Li J, et al. Inhibition of autophagy by 3-MA enhances the effect of 5-FU-induced apoptosis in colon cancer cells. Ann Surg Oncol. 2009;16:761–71. doi:10.1245/s10434-008-0260-0.
73. 10.1371/journal.pone.0056679
Pan X, et al. Autophagy inhibition promotes 5-fluorouraci-induced apoptosis by stimulating ROS formation in human non-small cell lung cancer A549 cells. *PLoS One* 2013, *8*, (e56679), doi:10.1371/journal.pone.0056679.
74. Itakura E, Mizushima N. Characterization of autophagosome formation site by a hierarchical analysis of mammalian Atg proteins. Autophagy. 2010;6:(764–776).
75. Russell RC, Yuan H-X, Guan K-L. Autophagy regulation by nutrient signaling. Cell Res. 2014;24:(42–57).

Figures

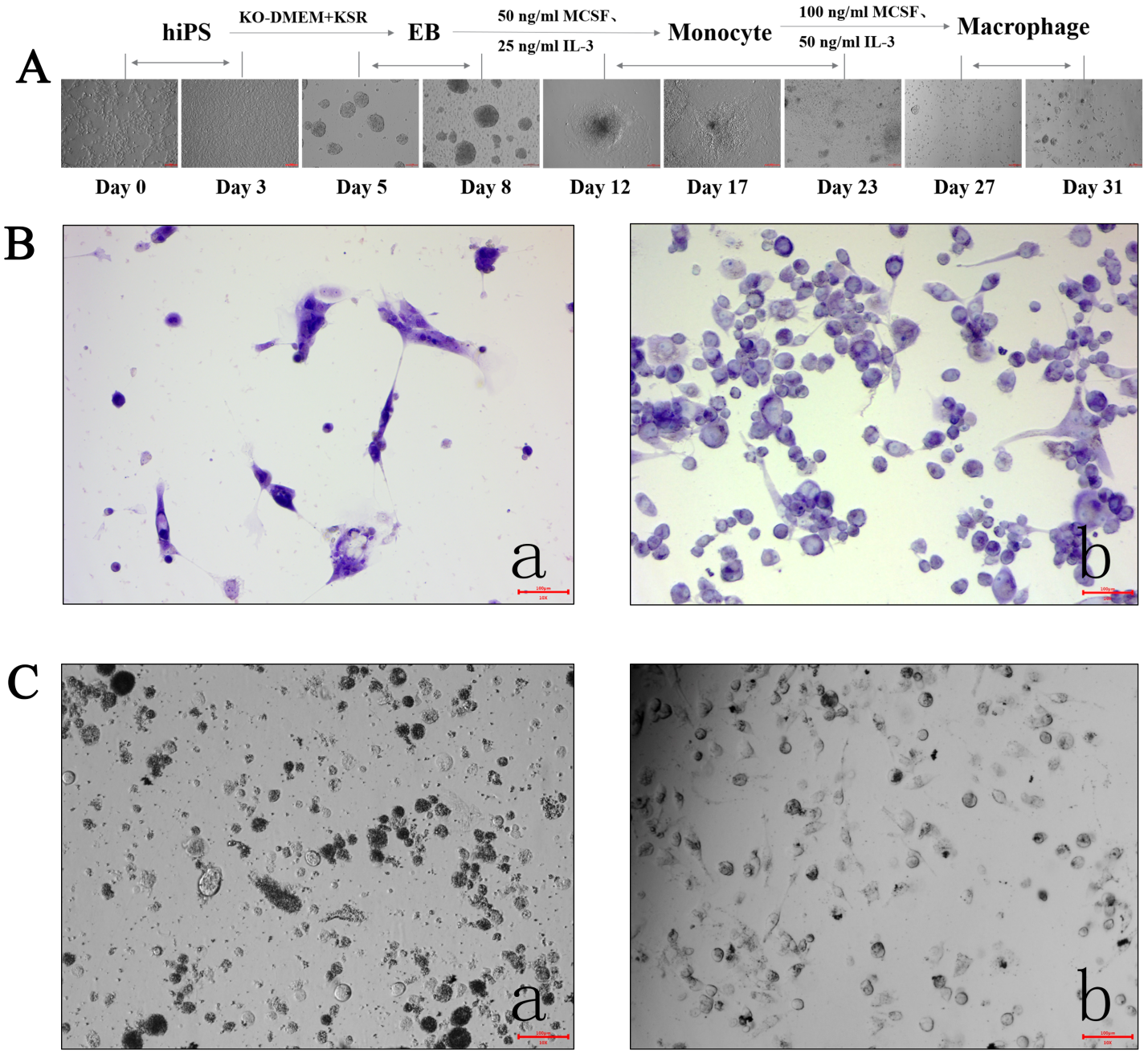

Figure 1

Functional characterization of hips-derived macrophages. (A) The process of hiPS differentiation into macrophages; (B) (a) The positive hiPS-Mφ cells after Gimesa stainning (Bar=100 μm), (b) The positive THP-1-Mφ cells after Gimesa stainning (Bar=100 μm); (C) (a) The positive hiPS-Mφ cells after phagocytic function test, indicating the macrophage-like cells of the source had a phagocytic function (Bar=100 μm), (b)The positive THP-1-Mφ cells after phagocytic function test, indicating the macrophage-like cells of the source had a phagocytic function (Bar=100 μm).

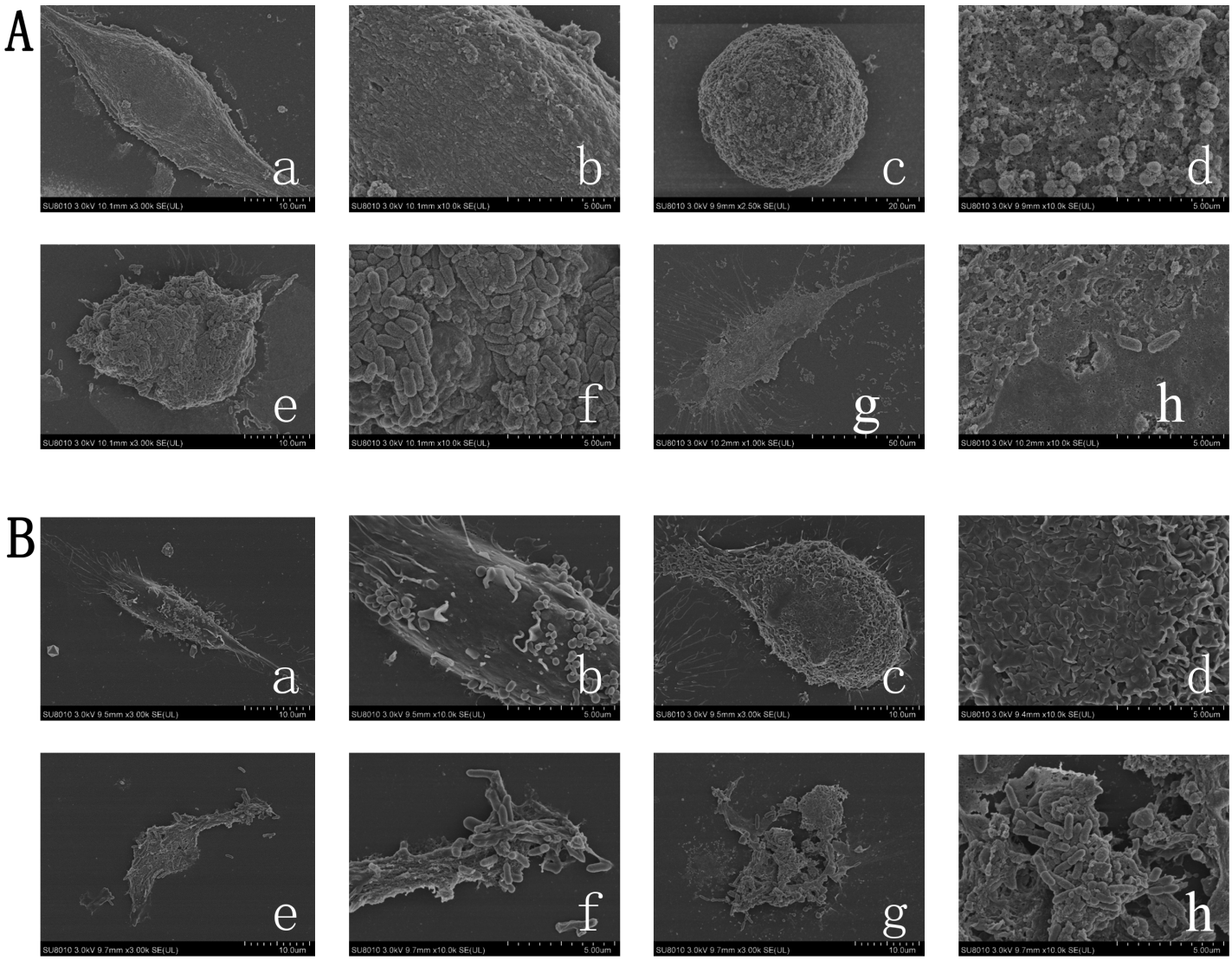

Figure 2

Submicroscopic observation of macrophages by SEM after 24 h infection with BCG. (A) Autophagy in hiPS-Mφ after 24 h BCG infection was observed by SEM, (a-d): (a) and (c) were hiPS-Mφ performed different morphology without BCG treatment, which were shown at higher magnification in (b) and (d) respectively; (e-h): (e) and (g) were hiPS-Mφ performed different morphology after BCG treatment, which were shown at higher magnification in (f) and (h) resepectively; (B) Autophagy in THP-1-Mφ after 24 h BCG infection was observed by SEM, (a-d): (a) and (c) were THP-1-Mφ performed different morphology without BCG treatment, which were shown at higher magnification in (b) and (d) respectively; (e-h): (e) and (g) were THP-1-Mφ performed different morphology after BCG treatment, which were shown at higher magnification in (f) and (h) resepectively. Without treatment, both of the hiPS-Mφ and THP-1-Mφ have typical morphology characteristics of Mφ, after 24 hours of BCG infection, the cells began to shrink, and severe lysis occurred. The distribution of rod-shaped bacteria was observed in the extracellular cells.

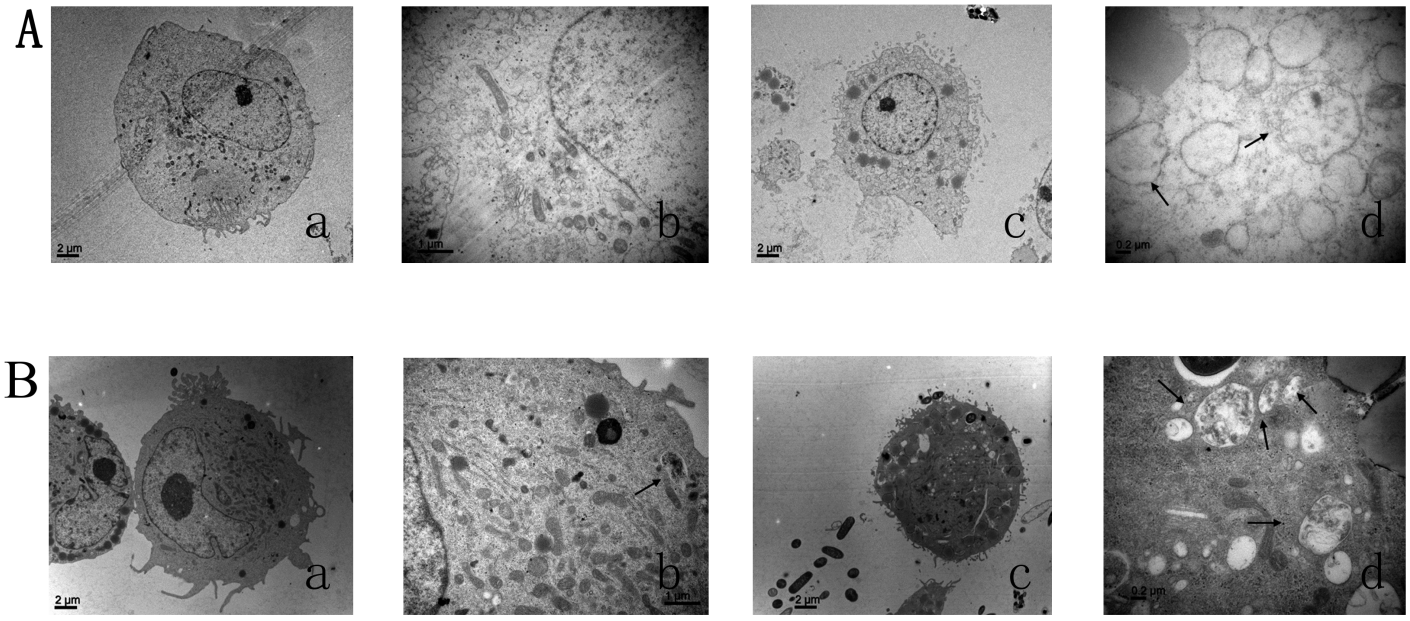

Figure 3

Submicroscopic observation of macrophages by TEM after 24 h infection with BCG . (A) Inconspicuous autophagy in hiPS-Mφ after 24 h BCG infection was observed by TEM, (a-b): (a) was hiPS-Mφ without treatment, which was shown at higher magnification in (b); (c-d): (c) was hiPS-Mφ treated with BCG, which was shown at higher magnification in (d). After 24 hours of BCG infection, the endoplasmic reticulum was obviously swollen and the number of autophagosomes increased, but it was not obvious. (B) Autophagy in THP-1-Mφ after 24 h BCG infection was observed by TEM,(a-b): (a) was THP-1-Mφ without treatment, which was shown at higher magnification in (b); (c-d): (c) was THP-1-Mφ treated with BCG, which was shown at higher magnification in (d). After 24 hours of BCG infection, the endoplasmic reticulum was obviously swollen and the number of autophagosomes increased.

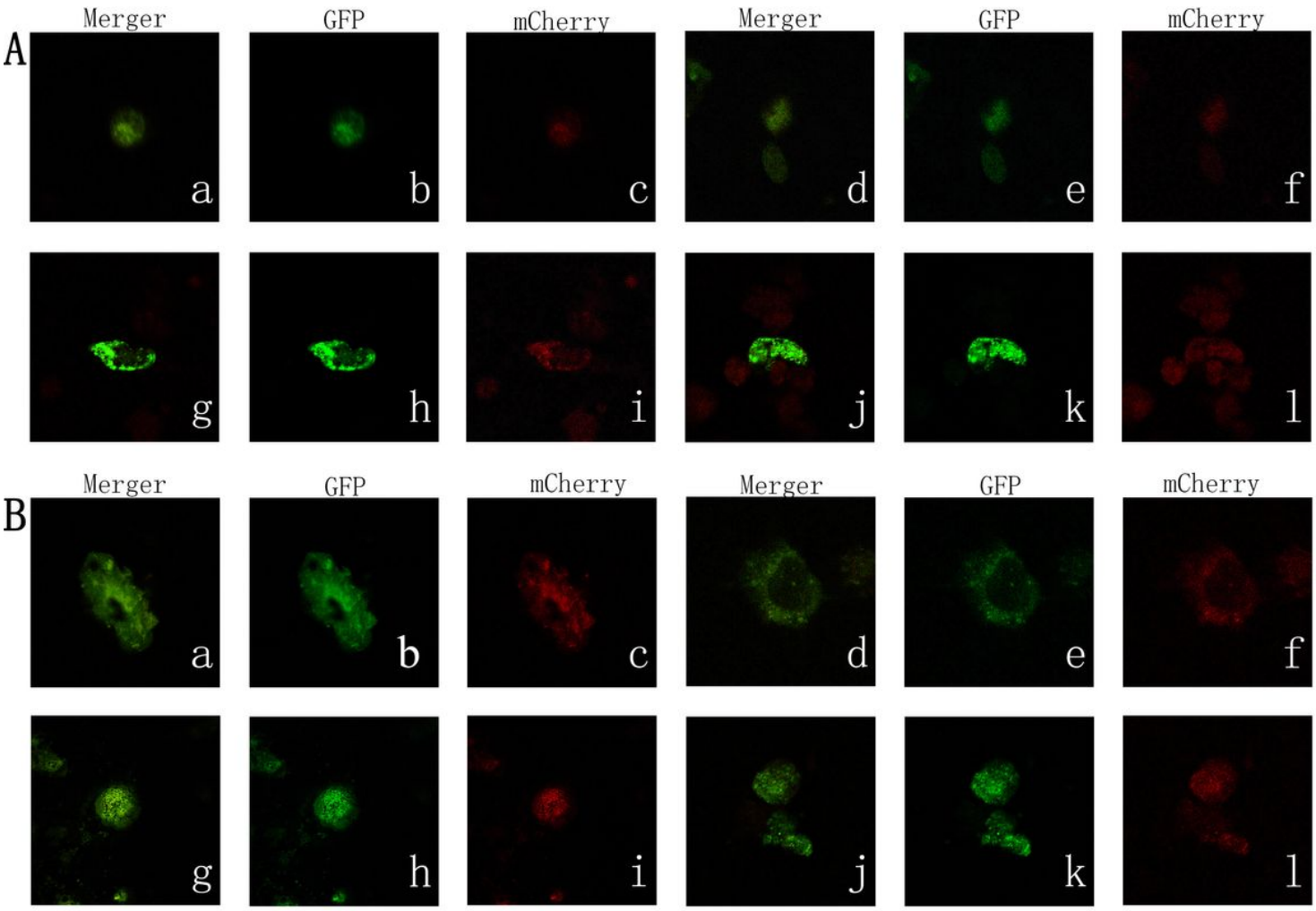

Figure 4

Laser confocal detection of autophagy after 24 h BCG infection of macrophages. (A) hiPS-Mφ were infected with Ad-mCherry-GFP-LC3B for 24 h and observed by laser confocal microscopy, MOI=20, (a-c): hiPS-Mφ, (d-f): hiPS-Mφ treated with 3-MA, (g-i): hiPS-Mφ treated with BCG, (j-l): hiPS-Mφ treated with 3-MA+BCG; (B) THP-1-Mφ were infected with Ad-mCherry-GFP-LC3B for 24 h and observed by laser confocal microscopy, MOI=20, (a-c): THP-1-Mφ, (d-f): THP-1-Mφ treated with 3-MA, (g-i): THP-1-Mφ treated with BCG, (j-l): THP-1-Mφ treated with 3-MA+BCG. The fluorescence of the control cells and the 3-MA-treated hiPS-Mφ and THP-1-Mφ cells were weak and diffusely presented in the cytoplasm, the number of intracellular autophagosomes is definitely small. The fluorescence of hiPS-Mφ and THP-1-Mφ cells in the BCG treatment group was mostly aggregated spots, and the fluorescence intensity was strong, the cells were autophagic, and the number of autophagosomes was high. The fluorescence expression of hiPS-Mφ and THP-1-Mφ cells in the 3-MA+BCG treatment group was similar to that in the BCG treatment group, except that the fluorescence intensity and the spots were slightly lower, the degree of autophagy was slightly lower than that of the BCG treatment group.

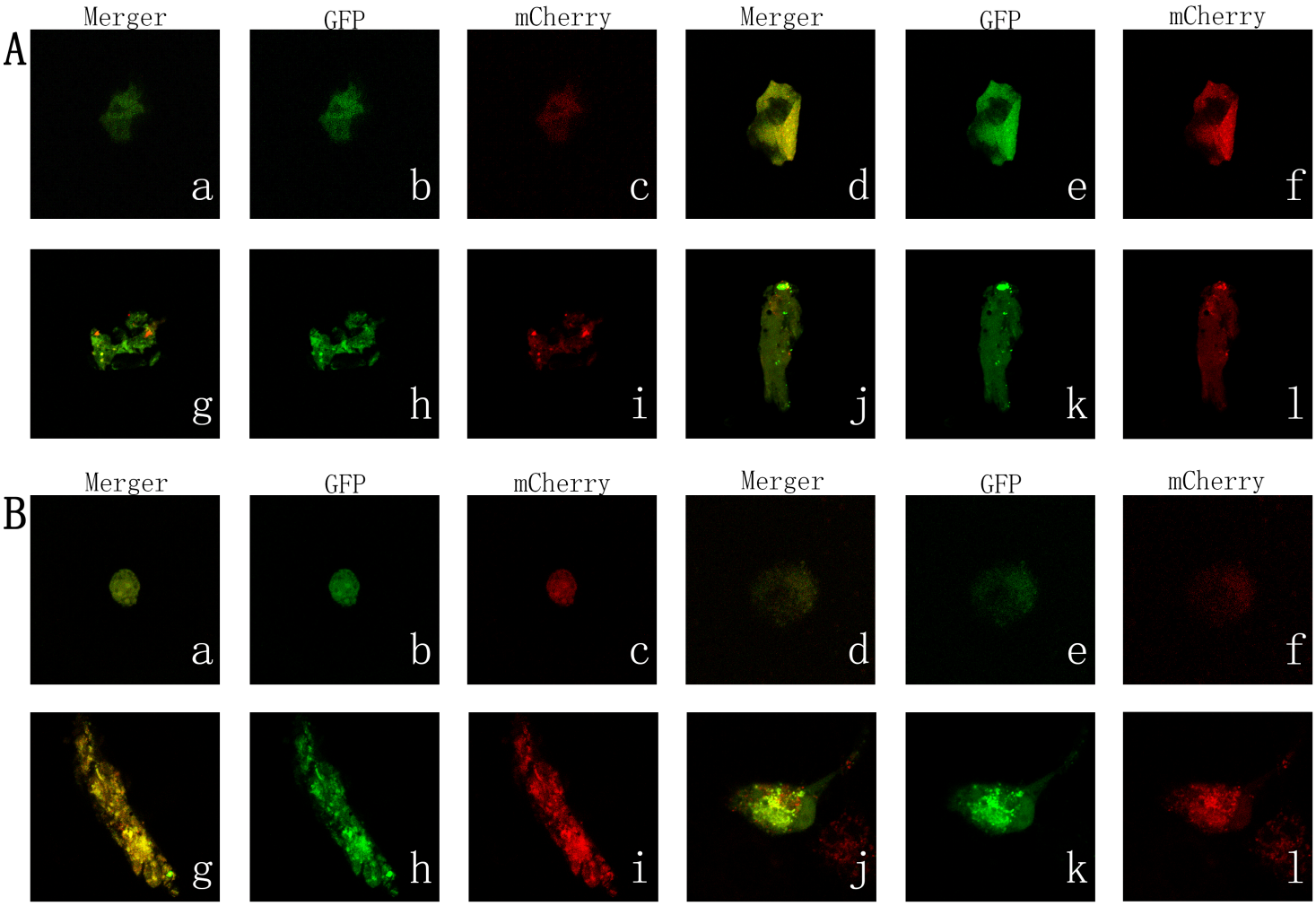

Figure 5

Laser confocal detection of autophagy after 48 h BCG infection of macrophages. (A) hiPS-Mφ were infected with Ad-mCherry-GFP-LC3B for 48 h and observed by laser confocal microscopy, MOI=20,(a-c): hiPS-Mφ without treatment, (d-f): hiPS-Mφ treated with 3-MA, (g-i): hiPS-Mφ treated with BCG, (j-l): hiPS-Mφ treated with 3-MA+BCG; (B) THP-1-Mφ were infected with Ad-mCherry-GFP-LC3B for 48 h and observed by laser confocal microscopy, MOI=20,(a-c): THP-1-Mφ without treatment, (d-f): THP-1-Mφ treated with 3-MA, (g-i): THP-1-Mφ treated with BCG, (j-l): THP-1-Mφ treated with 3-MA+BCG. Laser confocal microscopy showed that after infecting with Ad-mCherry-GFP-LC3B for 48 h, the fluorescence intensity of cells treated with different treatments was significantly increased than that of 24 h.

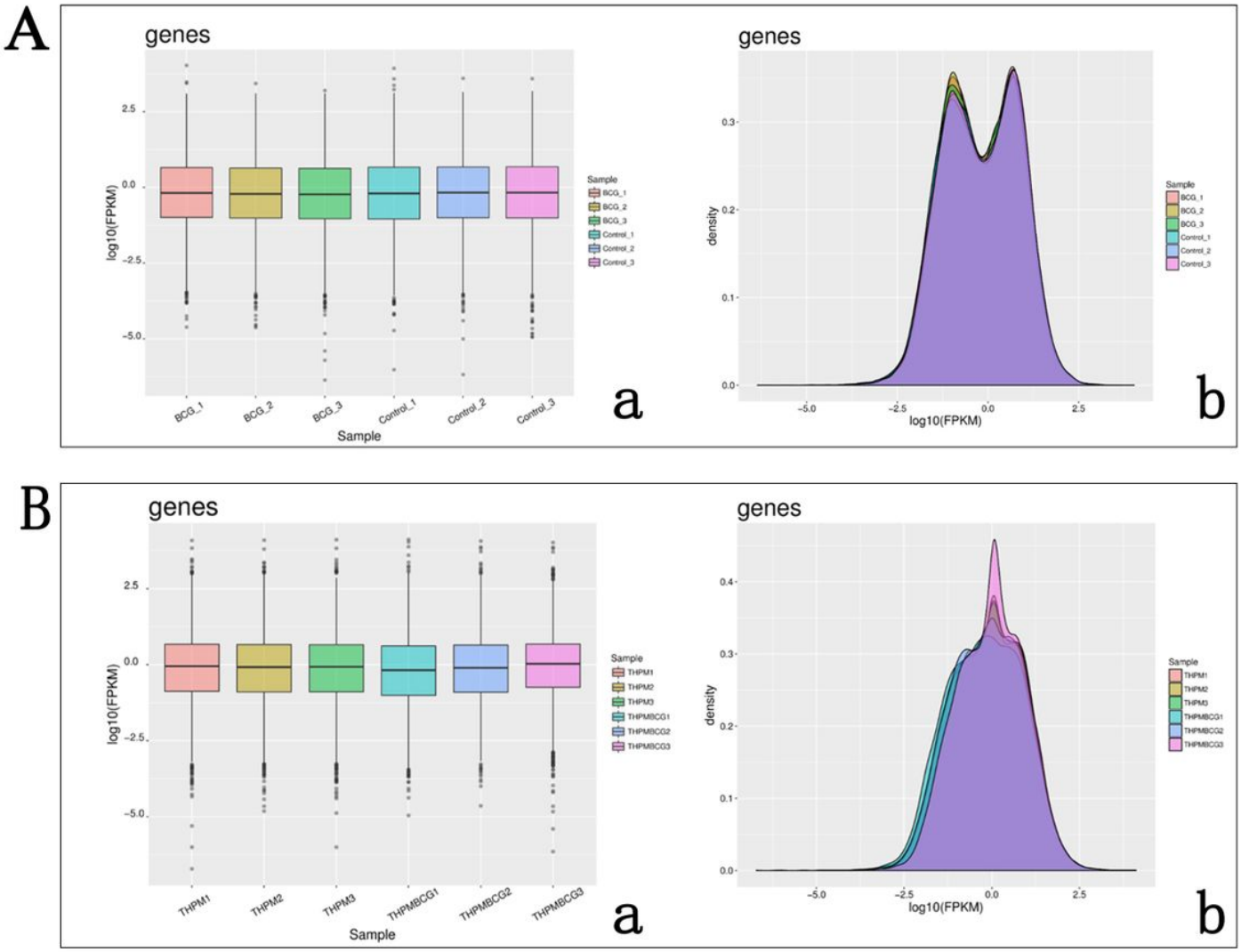

Figure 6

Distribution of hiPS-Mφ and THP-1-Mφ gene expression values.(A) hiPS-Mφ (a) hiPS-Mφ box plot, with the name of the sample as the abscissa and log 10 (FPKM) as the ordinate, the result proves that the sample has sample repeatability. (b) hiPS-Mφ expression value density map, with log10 (FPKM) as the abscissa and the density of genes as the ordinate. Mean values of three independent experiments are shown; (B)THP-1-Mφ (a) THP-1-Mφ box plot, with the name of the sample as the abscissa and log 10 (FPKM) as the ordinate, the result proves that the sample has sample repeatability. (b) THP-1-Mφ expression value density map, with log10 (FPKM) as the abscissa and the density of genes as the ordinate. Mean values of three independent experiments are shown.

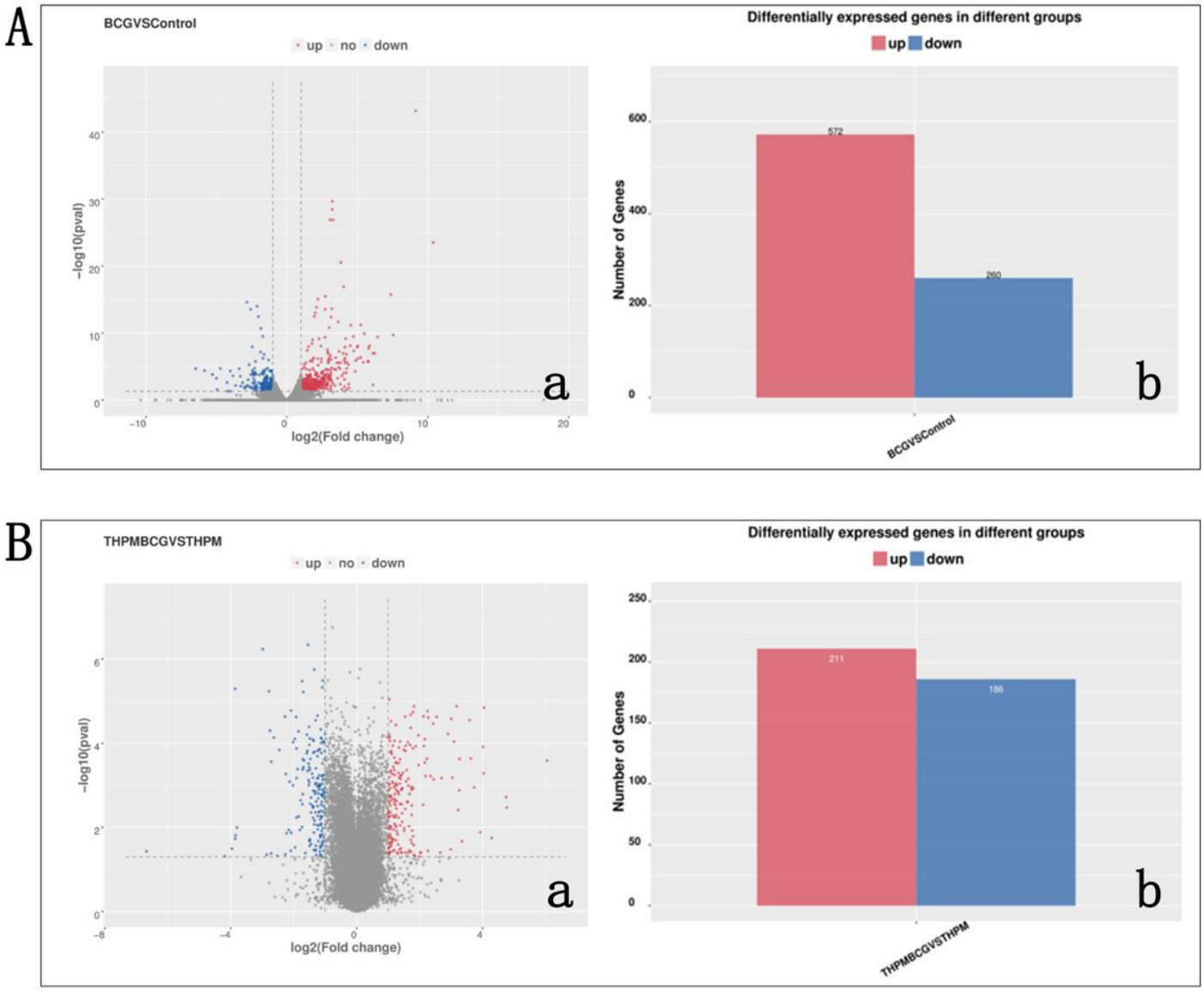

Figure 7

Differential gene expression of hiPS-Mφ and THP-1-Mφ. (A) hiPS-Mφ (a) hiPS-Mφ volcano map; (b) hiPS-Mφ histogram, with log2 (Fold Change, FC) as the abscissa and -log10 (p-value) as the ordinate, the statistical results showed that compared with the control hiPS-Mφ cells, BCG-treated hiPS-Mφ had 832 significantly differentially expressed genes, of which 572 genes were up-regulated and 260 genes were down-regulated. Mean values of three independent experiments are shown; (B) THP-1-Mφ (a) THP-1-Mφ volcano map; (b) THP-1-Mφ histogram, with log2 (Fold Change, FC) as the abscissa and -log10 (p-value) as the ordinate, compared with the control THP-1-Mφ cells, BCG-treated THP-1-Mφ had 397 significant differentially expressed genes, of which 211 genes were up-regulated and 186 genes were down-regulated.

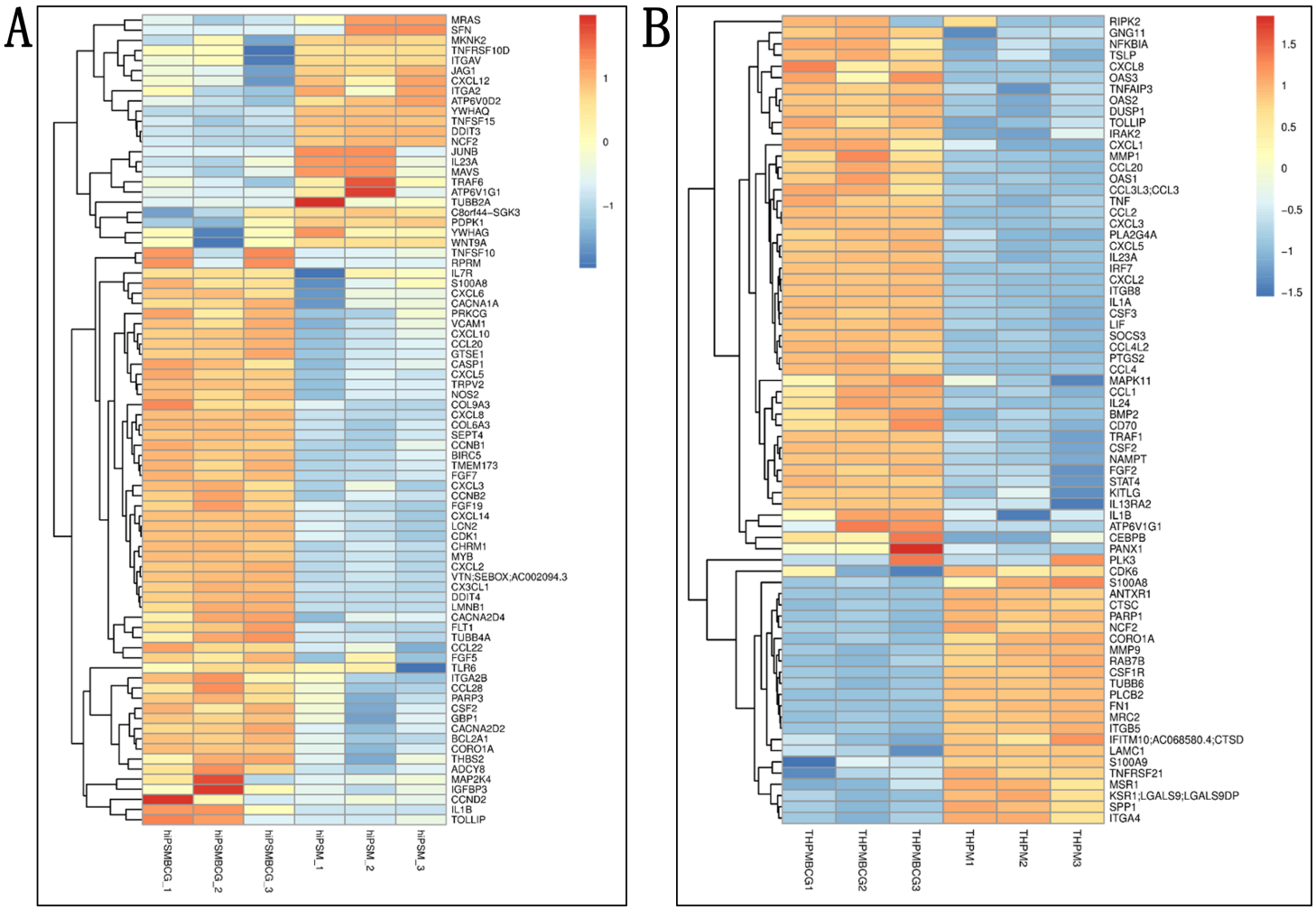

Figure 8

Heat map of hiPS-Mφ and THP-1-Mφ differential gene expression The abscissa is the sample name, the ordinate is the name of the differentially expressed gene, and the different colors express different gene expression levels. The color ranges from blue to white, then to red, indicating low to high expression, and red indicates high expression of genes while dark blue indicates a low expression gene. Mean values of three independent experiments are shown; (A) hiPS-Mφ; (B) THP-1-Mφ.

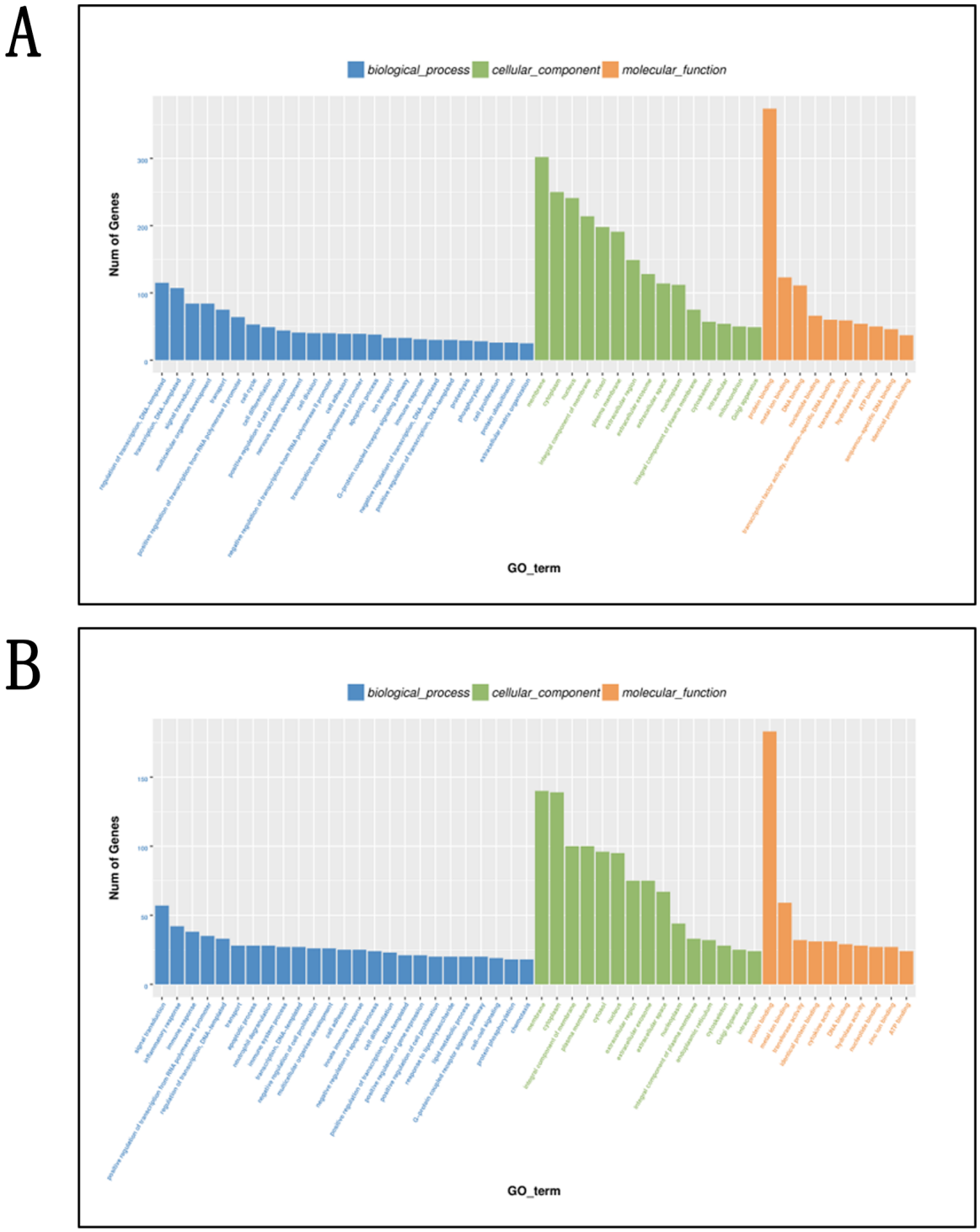

Figure 9

GO enrichment analysis of differentially expressed genes. The results indicate that it is mainly involved in processes such as transcriptional regulation, signal transduction, cell membrane composition, and protein binding. (A) hiPS-Mφ, in the hiPS-Mφ group, GO enrichment analysis of differentially expressed genes indicated that it is mainly involved in processes such as transcriptional regulation, signal transduction, cell membrane composition and protein binding; (B) THP-1-Mφ, in the THP-1-Mφ group, GO

enrichment analysis of differentially expressed genes indicated that it is mainly involved in signal transduction, inflammatory response, immune response, cell membrane composition and protein binding. Mean values of three independent experiments are shown.

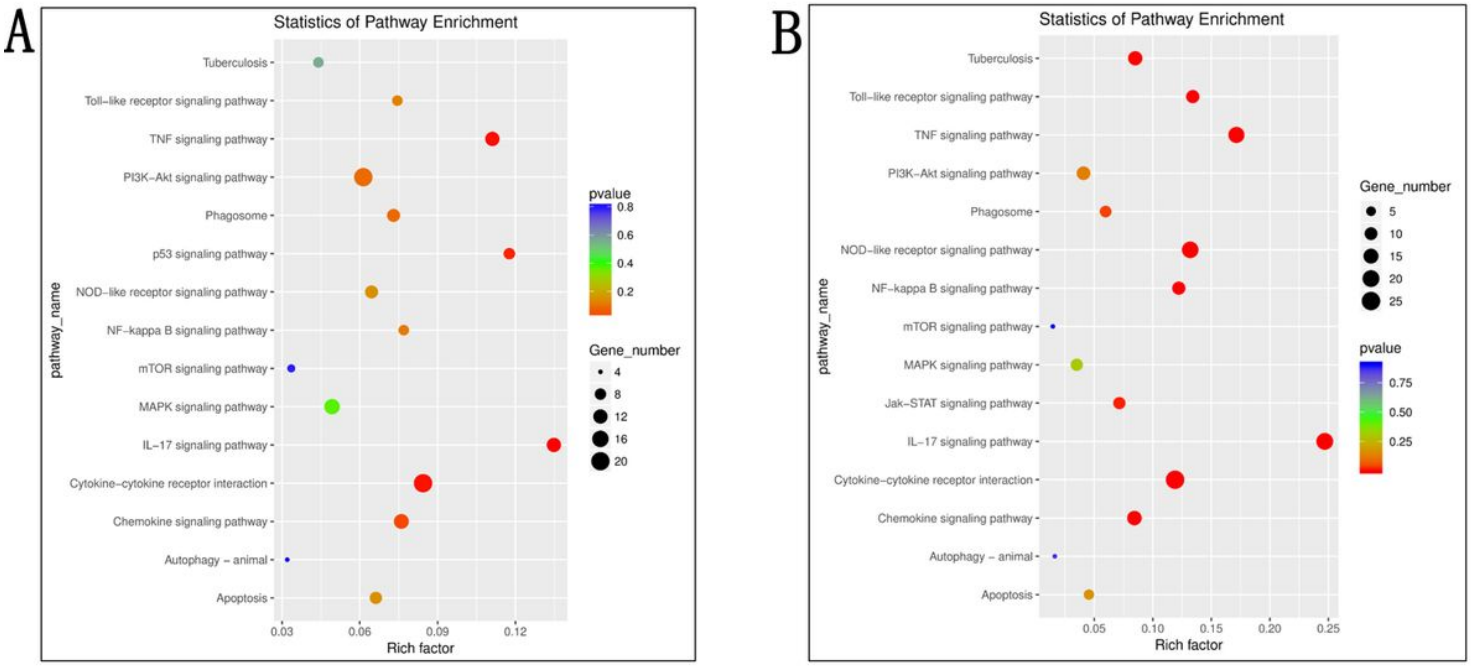

Figure 10

Scatter plot of KEGG enrichment analysis of hiPS-Mφ and THP-1- Mφ. It shows a partial integrative metabolic pathway for KEGG enrichment analysis of hiPS-Mφ and THP-1-Mφ after BCG treatment. (A) hiPS-Mφ, pathway of hiPS-Mφ associated with inflammation, autophagy, apoptosis, etc. after BCG treatment has significant changes; (B) THP-1-Mφ, pathway related to inflammation, autophagy, apoptosis, etc. of THP-1-Mφ after BCG treatment also changed significantly. Mean values of three independent experiments are shown.

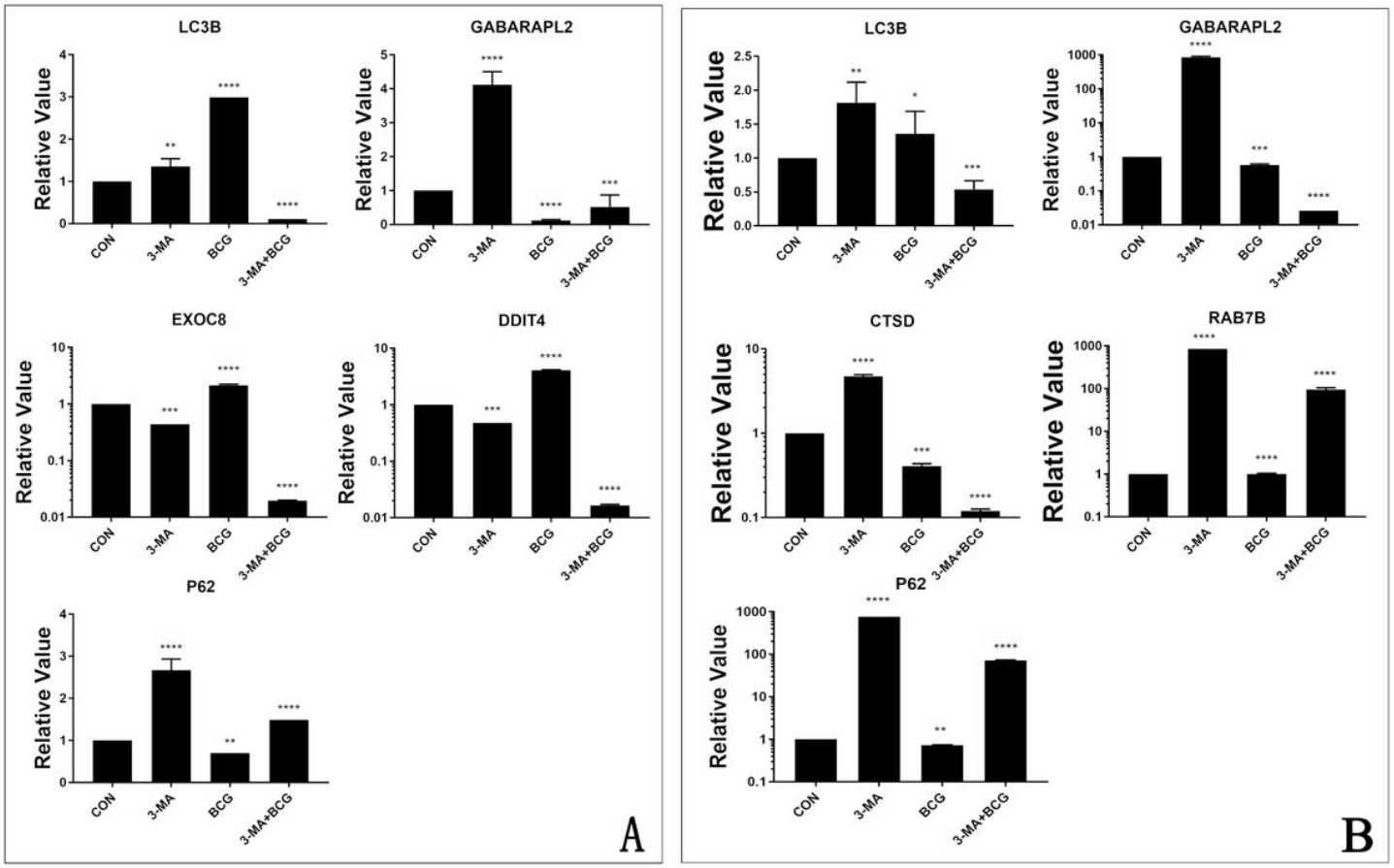

Figure 11

Expression of autophagy-related genes in hiPS-Mφ and THP-1-Mφ. (A)hiPS-Mφ, compared with uninfected hiPS-Mφ, the expression of LC3B was significantly increased after BCG infection with hiPS-Mφ, the expression of GABARAPL2 was significantly decreased, and the expression of P62 was significantly decreased, the expression of DDIT4 and EXOC8 was significantly increased after BCG infection with hiPS-Mφ; (B) THP-1-Mφ; compared with uninfected THP-1-Mφ, the expression of LC3B gene was significantly increased after BCG infection of THP-1-Mφ, the expression of GABARAPL2 gene was significantly decreased, and the expression of P62 gene was significantly decreased. Mean values of three independent experiments are shown. Error bars are ±SD of three independent experiments. Uncorrected Fisher's least significant differences test: ns, non-significant; *p < 0.05, **p < 0.01,***p < 0.001, ****p < 0.0001.

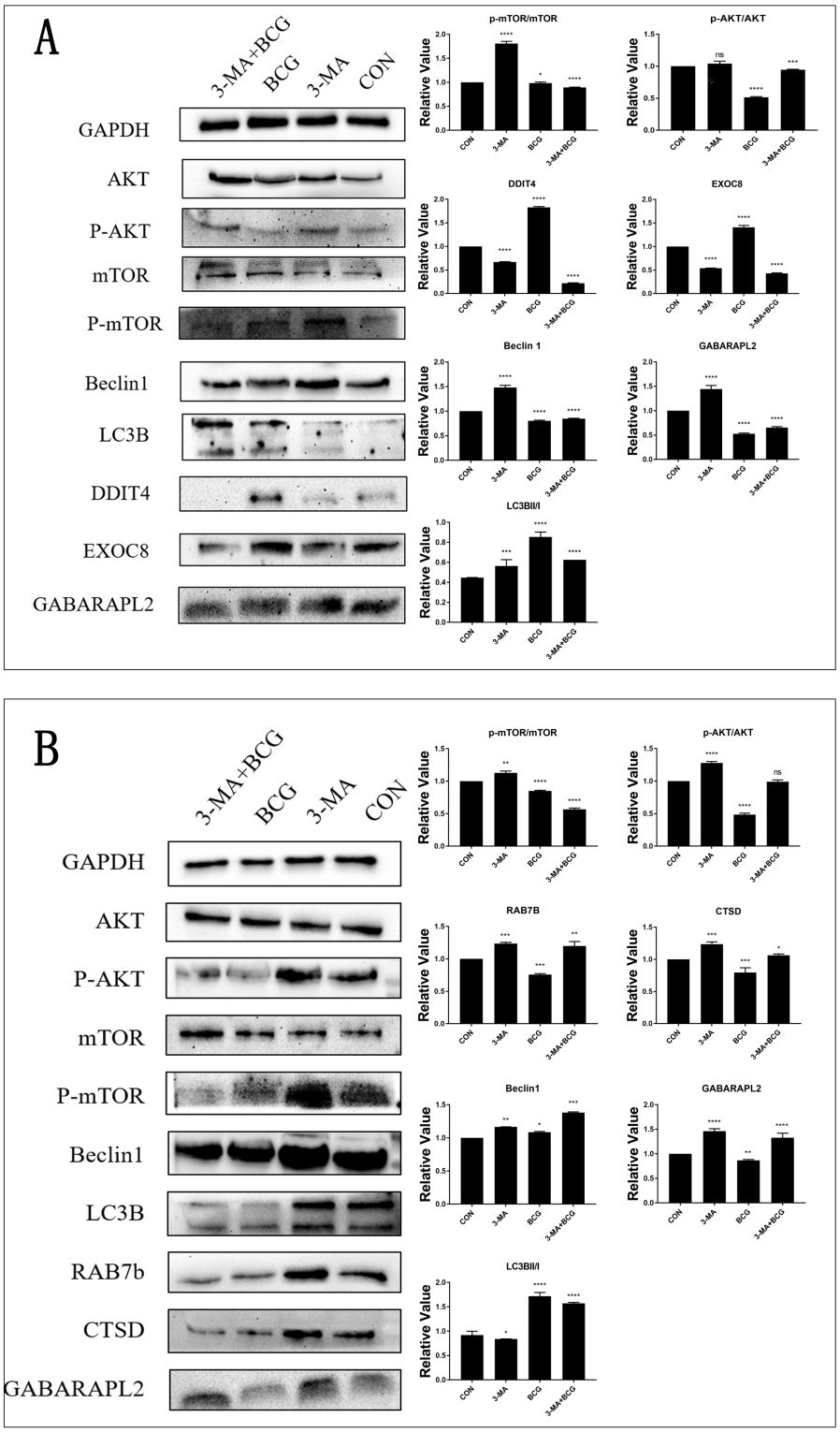

Figure 12

The effect of BCG on the expression of autophagy-related proteomes in hiPS-Mφ and THP-1-Mφ. (A) hiPS-Mφ, the expression of GABARAPL2, p-AKT, p-mTOR and Beclin1 in the hiPS-Mφ treated with BCG was significantly lower than that of the control group, and the ratio of LC3BII/I increased significantly, the expression of DDIT4 and EXOC8 was increased in the hiPS-Mφ treated with BCG; (B) THP-1-Mφ, the expression of GABARAPL2, p-AKT, p-mTOR and Beclin1 in the THP-1-Mφ treated with BCG was

significantly lower than that of the control group, and the ratio of LC3BII/I increased significantly, the expression of RAB7B and CTSD decreased after THP-1-Mφ treatment with BCG. Mean values of three independent experiments are shown. Error bars are ±SD of three independent experiments. Uncorrected Fisher's least significant differences test: ns, non-significant; *p < 0.05, **p < 0.01,***p < 0.001, ****p < 0.0001.

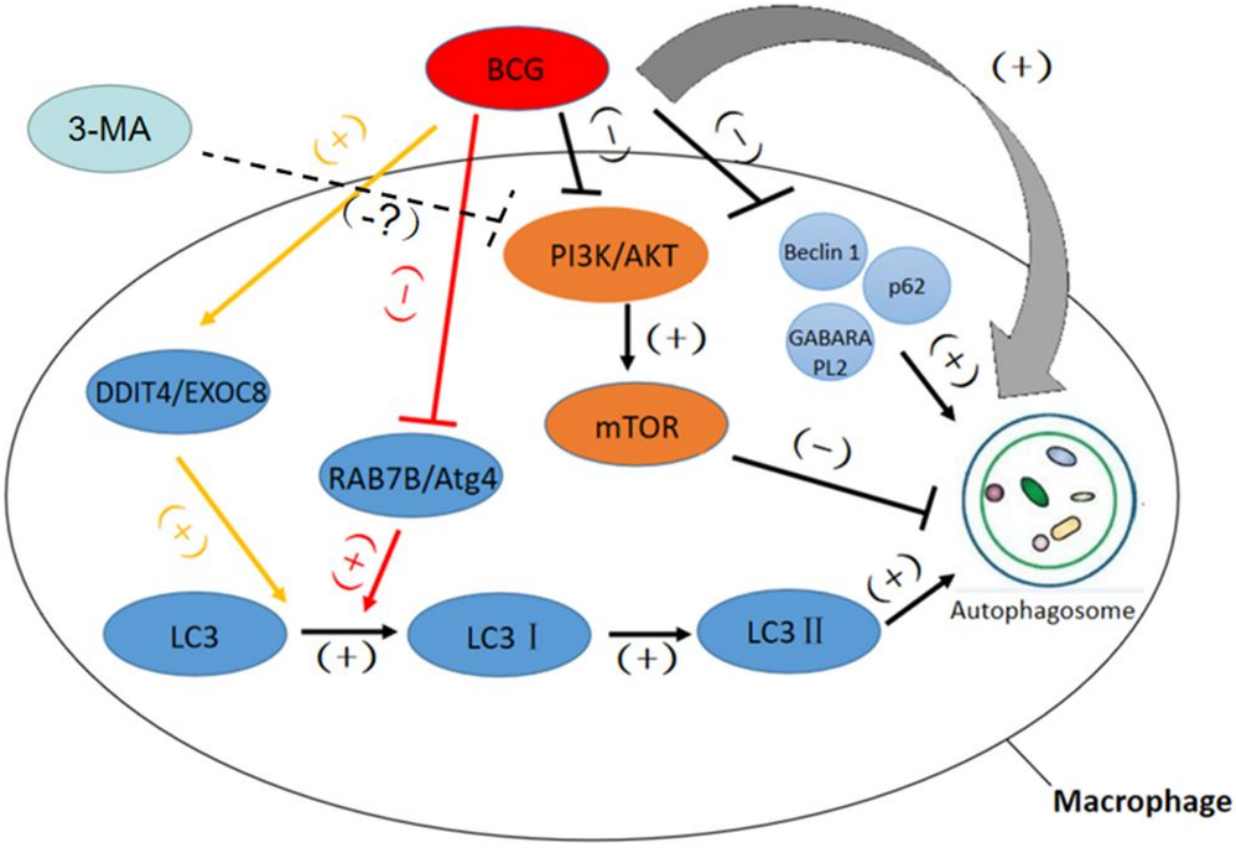

Figure 13

: Model of BCG-mediated expression levels of autophagy-associated genes by activation of the PI3K/AKT/mTOR signaling pathway in hiPS-Mφ and THP-1-Mφ, red lines indicate THP-1-Mφ and yellow lines indicate hiPS-Mφ, using 3-methyladenine as a constrast to BCG.